Title

Editor's Highlight: Congener-Specific Disposition of Chiral Polychlorinated Biphenyls in Lactating Mice and Their Offspring: Implications for PCB Developmental Neurotoxicity

Journal

Toxicological Sciences, 158(1)

ISSN

1096-6080

Authors

Kania-Korwel, Izabela

Lukasiewicz, Tracy

Barnhart, Christopher D

et al.

Publication Date

2017-07-01

DOI

10.1093/toxsci/kfx071

OXFORD

SOT | Society of Toxicology
www.toxsci.oxfordjournals.org

TOXICOLOGICAL SCIENCES, 158(1), 2017, 101–115

doi: 10.1093/toxsci/kfx071
Advance Access Publication Date: April 14, 2017
Research article

Congener-Specific Disposition of Chiral Polychlorinated Biphenyls in Lactating Mice and Their Offspring: Implications for PCB Developmental Neurotoxicity

Izabela Kania-Korwel,*,[2] Tracy Lukasiewicz,* Christopher D. Barnhart,†,[3] Marianna Stamou,†,[4] Haeun Chung,‡ Kevin M. Kelly,* Stelvio Bandiera,‡ Pamela J. Lein,† and Hans-Joachim Lehmler*,[1,2]

*Department of Occupational and Environmental Health, College of Public Health, The University of Iowa, Iowa City, Iowa; †Department of Molecular Biosciences, School of Veterinary Medicine, University of California, Davis, California; and ‡Faculty of Pharmaceutical Sciences, The University of British Columbia, Vancouver, British Columbia V6T 1Z3, Canada

[1]To whom correspondence should be addressed at Department of Occupational and Environmental Health, The University of Iowa, University of Iowa Research Park, no. 221 IREH, Iowa City, IA 52242-5000. Fax: (319) 335-4290. E-mail: hans-joachim-lehmler@uiowa.edu.

[2]Present address: Health Research Institute Laboratories, Fairfield, IA.

[3]Present address: Department of Molecular Pharmacology, Albert Einstein College of Medicine, Bronx, New York, NY.

[4]Present address: Department of Health Sciences and Technology, ETH Zürich, Zürich, Switzerland.

ABSTRACT

Chiral polychlorinated biphenyl (PCB) congeners have been implicated by laboratory and epidemiological studies in PCB developmental neurotoxicity. These congeners are metabolized by cytochrome P450 (P450) enzymes to potentially neurotoxic hydroxylated metabolites (OH-PCBs). The present study explores the enantioselective disposition and toxicity of 2 environmentally relevant, neurotoxic PCB congeners and their OH-PCB metabolites in lactating mice and their offspring following dietary exposure of the dam. Female C57BL/6N mice (8-weeks old) were fed daily, beginning 2 weeks prior to conception and continuing throughout gestation and lactation, with 3.1 μmol/kg bw/d of racemic 2,2′,3,5′,6-pentachlorobiphenyl (PCB 95) or 2,2′,3,3′,6,6′-hexachlorobiphenyl (PCB 136) in peanut butter; controls received vehicle (peanut oil) in peanut butter. PCB 95 levels were higher than PCB 136 levels in both dams and pups, consistent with the more rapid metabolism of PCB 136 compared with PCB 95. In pups and dams, both congeners were enriched for the enantiomer eluting second on enantioselective gas chromatography columns. OH-PCB profiles in lactating mice and their offspring were complex and varied according to congener, tissue and age. Developmental exposure to PCB 95 versus PCB 136 differentially affected the expression of P450 enzymes as well as neural plasticity (*arc* and *ppp1r9b*) and thyroid hormone-responsive genes (*nrgn* and *mbp*). The results suggest that the enantioselective metabolism of PCBs to OH-PCBs may influence neurotoxic outcomes following developmental exposures, a hypothesis that warrants further investigation.

Key words: atropisomer; chiral; cytochrome P450 enzymes; metabolites; persistent organic pollutants; polychlorinated biphenyls; plasticity.

PCBs are a class of 209 individual chemicals (or congeners) that represent a human health concern because of their ubiquitous presence in environmental samples (Lehmler *et al.*, 2010) and human tissues (Kania-Korwel and Lehmler, 2016b; Megson *et al.*, 2013; Mitchell *et al.*, 2012; Whitcomb *et al.*, 2005; Wingfors *et al.*, 2006). Human exposure to PCBs occurs *via* the diet (Schecter

et al., 2010; Shin et al., 2015) and inhalation of outdoor and indoor air (Grimm et al., 2015; Jamshidi et al., 2007). Epidemiological data suggest a negative association between developmental exposure to environmental PCBs and neuropsychological and cognitive function in infancy and childhood (Jacobson and Jacobson, 1996; Korrick and Sagiv, 2008; Nowack et al., 2015), but the mechanisms underlying the developmental neurotoxicity of PCBs, as well as the relative contribution of each congener to neurotoxic outcomes, remain poorly characterized. In particular, PCB congeners with *ortho*-chlorine substituents such as PCB 95 (2,2′,3,5′,6-pentachlorobiphenyl) and PCB 136 (2,2′,3,3′,6,6′-hexachlorobiphenyl) have emerged as developmental neurotoxicants of concern because they are present in indoor air in U.S. schools (Thomas et al., 2012) and have been detected at higher levels in children compared with older participants in the National Health and Nutrition Examination Survey (Megson et al., 2013). Moreover, levels of PCB 95, but not other PCBs, were higher in postmortem brain samples from individuals with neurodevelopmental disorders compared with neurotypical controls (Mitchell et al., 2012).

Laboratory studies using individual PCB congeners or PCB mixtures demonstrate that developmental PCB exposure causes behavioral and cognitive deficits in rats and mice (Boix et al., 2011; Cauli et al., 2013; Schantz et al., 1995; Yang et al., 2009). Several of these PCB congeners, such as PCB 95 and PCB 136, are potent sensitizers of ryanodine receptors (RyRs) (Pessah et al., 2006), which are important microsomal Ca^{2+} channels implicated in PCB-mediated developmental neurotoxicity (Kodavanti and Curras-Collazo, 2010; Pessah et al., 2010). PCB 95 and PCB 136 are chiral PCB congeners and exist as rotational isomers, called atropisomers, which are nonsuperimposable mirror images of each other (Lehmler et al., 2010). Racemic PCB 95 promotes dendritic growth *in vivo* and *in vitro via* RyR-mediated mechanisms (Wayman et al., 2012b). These effects of PCB 95 on dendritic growth are mediated by Ca^{2+}-dependent signaling pathways that regulate activity-dependent dendritic growth and synaptogenesis (Lesiak et al., 2014; Wayman et al., 2012a). *In vitro* studies demonstrate that chiral PCB 136 enantiospecifically affects dendritic growth by mechanisms involving RyRs, with (−)-PCB 136, but not (+)-PCB 136 activating RyRs to enhance dendritic arborization in primary neurons (Pessah et al., 2009; Yang et al., 2014). It is likely that other chiral PCB congeners also enantioselectively activate RyRs, but this has not yet been demonstrated experimentally.

PCBs are metabolized by cytochrome P450 (P450) enzymes to complex mixtures of hydroxylated PCBs (OH-PCBs) (Grimm et al., 2015). Animal studies demonstrate that these metabolites can cross the placenta and accumulate in fetal tissues (Meerts et al., 2002; Morse et al., 1995). In the case of PCB 136, OH-PCB metabolites are retained in the rat fetus due to their conjugation to the corresponding glucuronide (Lucier et al., 1978). There is also indirect evidence that OH-PCBs cross the placenta in humans and achieve higher levels in the fetus relative to the parent PCBs (Park et al., 2007; Soechitram et al., 2004). OH-PCB metabolites are potentially toxic (Grimm et al., 2015) and several studies demonstrate that some OH-PCBs cause developmental neurotoxicity by disrupting thyroid hormone or sex hormone homeostasis (Meerts et al., 2002, 2004a,b; Morse et al., 1995). OH-PCB metabolites of RyR-active PCBs are also potent sensitizers and uncouplers of RyRs (Niknam et al., 2013; Pessah et al., 2006) and may contribute to adverse behavioral outcomes in laboratory models and humans. However, limited information about the disposition of RyR-active OH-PCBs in dams and their offspring is currently available.

This study explores the enantioselective disposition of PCB 95 and PCB 136 and their OH-PCB metabolites in preweanling mice that were exposed to individual PCB congeners during gestation and lactation *via* the maternal diet. Our results establish that metabolism of both PCB 95 and PCB 136 results in congener-specific enantiomeric enrichment and complex OH-PCB profiles in brain and other tissues in pups and dams. Maternal exposure to RyR-active PCBs alters the hepatic expression of P450 enzymes as well as neural plasticity and thyroid-hormone responsive genes in the brains of offspring, suggesting the need for future studies to determine how the enantioselective formation of RyR-active OH-PCBs alters the developmental neurotoxicity of PCBs.

MATERIALS AND METHODS

Chemicals. 2,2′,3,5′,6-Pentachlorobiphenyl (PCB 95; lot 010610KS, 99.7% purity), 2,2′,3,3′,6,6′-hexachlorobiphenyl (PCB 136; lot 11993, 99.9% purity), 2,3,4′,5,6-pentachlorobiphenyl (PCB 117; 99% purity), 2,2′,3,4,4′,5,6,6′-octachlorobiphenyl (PCB 204; 99.9% purity) and 2,3,3′,4,5,5′-hexachlorobiphenyl-4′-ol (4′-159, >99.9% purity) were purchased from AccuStandard (New Haven, Connecticut, USA). Hydroxylated or methoxylated derivatives, including 3-methoxy-2,2′,4,5′,6-pentachlorobiphenyl (3-103), 3-methoxy-2,2′,3′,4,6,6′-hexachlorobiphenyl (3-150), 2,2′,3,5′,6-pentachlorobiphenyl-4-ol (4-95), 2,2′,3,3′,6,6′-hexachlorobiphenyl-4-ol (4-136), 2,2′,3,5′,6-pentachlorobiphenyl-5-ol (5-95), 2,2′,3,3′,6,6′-hexachlorobiphenyl-5-ol (5-136), 4,5-dimethoxy-2,2′,3,5′,6-pentachlorobiphenyl (4,5-95) and 4,5-dimethoxy-2,2′,3,3′,6,6′-hexachlorobiphenyl (4,5-136), were synthesized at >95% purity as described previously in Joshi et al. (2011), Kania-Korwel et al. (2008b), and Waller et al. (1999).

Animals and PCB exposure. Ten male and twenty female C57BL/6N mice at 7 weeks of age were purchased from Charles River Laboratories (Roanoke, Illinois, USA). Mice were maintained on a 12-h light, 12-h dark cycle, and at 20 to 26 °C in an AAALAC accredited animal facility at the University of Iowa Research Park (Coralville, Iowa, USA). Mice were housed in polypropylene, fiber-covered cages in HEPA-filtered Thoren caging units (Hazelton, Pennsylvania, USA) with SoftZorb Enrichment Blend bedding from NEPCO (Warrensburg, New York, USA). Food (sterile Teklad 5% stock diet, Harlan, Madison, Wisconsin, USA) and water (*via* an automated watering system) were provided *ad libitum*. Daily animal welfare-assessments were performed by laboratory personnel and no adverse outcomes were observed throughout the study. Animals were treated according to protocols approved by the Institutional Animal Care and Use Committee of the University of Iowa.

The dosing regimen for this study was adopted from earlier reports investigating PCB developmental neurotoxicity in rats (Schantz et al., 1997; Yang et al., 2009) and the enantioselective disposition of racemic PCB 95 in mice (Kania-Korwel et al., 2012, 2015). Briefly, female mice were exposed daily for 1 week to organic peanut oil (12.5 ml/g; Spectrum Organic Products; Melville, New York, USA) mixed with organic peanut butter (Trader Joe's; Monrovia, California, USA) as shown in Figure 1 (Kania-Korwel et al., 2012). Afterwards, animals were randomly divided into 3 exposure groups and treated daily throughout the study by dietary exposure to racemic PCB 95 (1.0 mg/kg bw/d; 3.1 μmol/kg bw/d; 7 females mated, 5 with and 2 without litters), racemic PCB 136 (1.1 mg/kg bw/d; 3.1 μmol/kg bw/d; 7 females mated, 6 with and 1 without litters) or vehicle alone (peanut oil, 12.5 ml/g peanut butter; 6 females mated, 5 with and 1 without

litters) in peanut butter. This PCB dosage was selected because PCB exposure at this dosage causes neurodevelopmental deficits in rats by mechanisms involving sensitization of the RyR (Schantz *et al.*, 1997; Wayman *et al.*, 2012b). Mice were weighed daily (Supplementary Figure 1) and the amount of peanut butter was adjusted to keep the PCB dosage constant. Exposure continued for 2 weeks before female mice were mated with male C57BL/6 mice for 3 days as described earlier in Kania-Korwel *et al.* (2012, 2015). Female mice that did not become pregnant (n = 4) were euthanized 3 weeks after mating by CO_2 asphyxiation followed by cervical dislocation. Exposure of pregnant female mice continued throughout gestation and lactation.

The number of pups was culled to 6 per litter on postnatal day 3 (P3), and the carcasses of P3 pups were stored at −80 °C. One male and one female pup from each litter were euthanized by decapitation on P7, the brain was excised, and tissue samples (ie, carcass and brain) were stored at −80 °C. The remaining pups (4 per litter) and dams were euthanized on P21 as described earlier for nonpregnant mice. Blood and tissues (brain, liver and muscle from the left hind leg) were collected from 1 male and 1 female P21 pup from each litter and stored at −80 °C for PCB analysis. Small samples of liver and brain from these pups and their dams were placed overnight in RNAlater (Qiagen, Valencia, California, USA) and stored at −80 °C for RNA extraction. Liver microsomes were prepared from the remaining male and female P21 pups by differential centrifugation as described previously in Kania-Korwel *et al.* (2008a) and stored in 0.25M sucrose at −80 °C.

Simultaneous extraction of PCB and metabolites from tissues. Blood (0.03–1.26 g), brain (0.09–0.49 g), carcass (1.66–4.9 g), liver (0.21–0.69 g) and muscle (0.02–0.18 g) samples were extracted and cleaned-up *in situ* with Florisil (12 g) using an Accelerated Solvent Extractor (ASE 200, Dionex, Sunnyvale, California) as reported earlier in Kania-Korwel *et al.* (2012). A hexane:dichloromethane:methanol mixture (48:43:9, *v/v/v*) was used as extraction solvent. Extracts were concentrated under a gentle stream of nitrogen and hydroxylated metabolites were derivatized to methoxylated compounds using a solution of diazomethane in diethyl ether. After removal of excess diazomethane, extracts were subjected to sulfur and sulfuric acid clean-up steps as described elsewhere (Kania-Korwel *et al.*, 2007).

Gas chromatographic analysis. Tissue levels of PCBs and their hydroxylated metabolites were simultaneously quantified on a SPB 1 column (60 m × 250 μm × 0.25 μm; Supelco, St Louis, Missouri, USA) using an Agilent 7870A gas chromatograph equipped with ^{63}Ni μ-electron capture detector (ECD) as described previously in Kania-Korwel *et al.* (2012). PCB and OH-PCB levels were determined using PCB 204 as an internal standard (volume corrector). PCB and OH-PCB levels are reported on a molar or weight basis and (1) adjusted for tissue wet weight or (2) expressed as total amount in the respective organ (Supplementary Tables 1–8). No lipid adjustments were made because hydroxylated PCB metabolites are more polar than PCBs and not associated with lipids (Guvenius *et al.*, 2003). Levels of PCB and OH-PCB expressed as nmol/g wet weight are compared throughout the manuscript to facilitate comparisons between the PCB exposure groups (see also Supplementary Tables 1 and 2 for data expressed as pmol/g). In addition, PCB and OH-PCB levels expressed as ng/g wet weight are presented in Supplementary Tables 3 and 4. Although wet weight adjusted PCB and OH-PCB levels are a good measure of their levels at target site(s) within the developing brain, we also expressed and analyzed the data as total amount per organ to assess the extent to which growth dilution may have contributed to age-related differences in PCB and OH-PCB levels (Supplementary Tables 5–8; Supplementary Figs. 2–6). PCB and OH-PCB levels and enantiomeric fractions (EFs) from male and female pups for the same litter were combined because we observed no statistically significant sex differences, consistent with previous reports of PCB developmental neurotoxicity (Dziennis *et al.*, 2008; Yang *et al.*, 2009).

EF values are a measure of the enantiomeric enrichment of a chiral compound and were determined for PCB 95, PCB 136 and 2 OH-PCB metabolites, 4-95 and 5-136, on an Agilent 7890 gas chromatograph equipped with a ^{63}Ni μ-ECD as described previously in Kania-Korwel *et al.* (2011, 2012). The following enantioselective columns were used: Chirasil-Dex column (CD, 2,3,6-tri-O-methyl-β-cyclodextrin, 30 m × 250 μm × 0.39 μm, Agilent, Santa Clara, California, USA) for PCB 136 and 5-136; BGB-172 column (BGB, 20% *tert*-butyldimethyl-silyl-β-cyclodextrin, 30 m × 250 μm × 0.25 μm, BGB Analytics, Boecten, Switzerland) for 4-95; and ChiralDex B-DM column (2,3-di-O-methyl-6-*tert*-butyl-silyl-β-cyclodextrin, 30 m × 250 μm × 0.12 μm, Supelco) for PCB 95. The remaining OH-PCB metabolites either co-eluted with other metabolites, were not resolved under the analysis conditions used in this study or were below the limit of detection in the enantioselective analysis (Kania-Korwel *et al.*, 2008b, 2011). All integrations were performed using the valley drop method (Kania-Korwel *et al.*, 2012). EF values were calculated as $EF = A_1/(A_1+A_2)$, where A_1 and A_2 are the peak area of the first (E_1) and second (E_2) eluting peak, respectively, and are summarized in Supplementary Table 9.

Quality assurance/quality control. The detector responses were linear from 1 ng to 1 μg for all analytes investigated (PCBs 95, 117, 136, 3-103, 5-95, 4′-95, 4-95, 4,5-95, 3-150, 4-136, 4,5-136, 4′-159), with R^2 values ≥ 0.995. Instrument detection limits, method detection limits and background levels in vehicle-treated animals are presented in Supplementary Table 10. Recoveries of the surrogate recovery standards added to each sample before extraction were 100% ± 11% (range: 52%–139%) and 81% ± 17% (range: 10% to 121%) for PCB 117 and 4′-159, respectively.

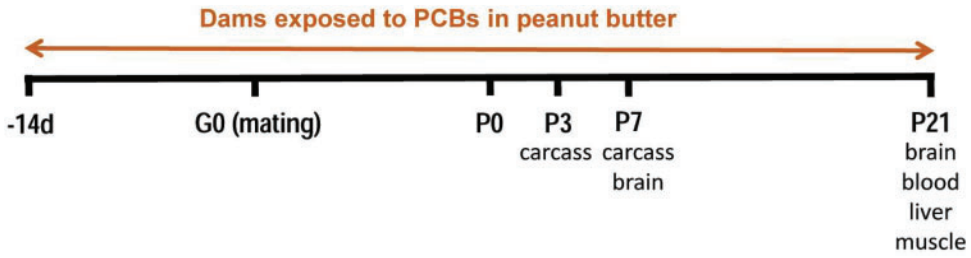

FIG. 1. Experimental design of the animal study showing time points at which tissue samples were collected to determine levels of parent PCBs and OH-PCBs.

RNA isolation and qPCR. Total RNA extraction from tissues, cDNA synthesis and quantitative polymerase chain reaction (qPCR) were performed by the Real-Time PCR Research and Diagnostics Core Facility at the University of California, Davis (Davis, California) using Taqman technology on a 7900HT Fast Real-Time PCR System (Applied Biosystems, Grand Island, New York, USA). Each cDNA sample was loaded in duplicate onto MicroAmp Optical 384-well plates (Life Technologies, Grand Island, New York, USA). Primer and probe sets were designed in-house, synthesized by Integrated DNA Technologies (Coralville, Iowa, USA) as previously described in Kania-Korwel *et al.* (2012) and are presented in Supplementary Table 11. Amplification efficiencies are provided in Supplementary Table 12. Transcript levels of *cyp1a2*, *cyp2b10*, and *cyp3a11* were normalized against the transcript level of the reference gene, phosphoglycerate kinase 1 (*pgk1*) (Santos and Duarte, 2008; Stamou *et al.*, 2014). Transcript levels of activity-regulated cytoskeleton-associated protein (*arc*), myelin basic protein (*mbp*), RC3/neurogranin (*nrgn*), and spinophilin (*ppp1r9b*) were normalized against the geometric mean of the transcript levels of the reference genes, *pgk1*, peptidylprolyl isomerase A (*ppia*), and hypoxanthine-guanine phosphoribosyl transferase (*hprt*) (Stamou *et al.*, 2014, 2015; Wu *et al.*, 2015).

Immunoblot analysis of P450 protein levels. Hepatic mouse P450 enzymes were identified and protein levels were measured by immunoblot analysis as described previously in Hrycay *et al.* (2014). Liver microsomal proteins were resolved by discontinuous sodium dodecyl sulfate polyacrylamide gel electrophoresis (SDS-PAGE) according to a published procedure (Laemmli, 1970). Liver microsomes prepared from individual dams and P21 pups were loaded on the gels at a concentration of 20 or 40 μg microsomal protein/lane. A single concentration of the appropriate purified rat P450 protein was included on each gel as an internal standard. The internal standard for blots probed with antirat CYP1A serum was rat CYP1A2, which was loaded at 0.1 pmol/lane; for blots probed with antirat CYP2B IgG, purified rat CYP2B2 at 0.0625 pmol/lane; for blots probed with antirat CYP3A IgG, CYP3A2 at 0.5 pmol/lane. Proteins separated by SDS-PAGE were transferred electrophoretically onto nitrocellulose membranes as reported earlier (Towbin *et al.*, 1979). The membranes were incubated for 2 h at 37 °C with rabbit antirat CYP1A serum at 1:1000 dilution, rabbit antirat CYP2B1 IgG at 5 μg/ml or rabbit antirat CYP3A IgG at 15 μg/ml. The primary antibodies were prepared in house, as described previously in Ngui and Bandiera (1999) and Wang and Bandiera (1996). Membranes were then washed and incubated for 2 h at 37 °C with alkaline phosphatase-conjugated goat $F(ab')_2$ antirabbit IgG (Jackson ImmunoResearch Laboratories, West Grove, Pennsylvania, USA; Cat no. 111-056-047, RRID:AB_2337957) at a dilution of 1:3000. Membranes were washed again and protein bands visualized by incubation with a substrate solution consisting of 0.03% *p*-nitroblue tetrazolium chloride and 0.015% 5-bromo-4-chloro-3-indolyl phosphate in 0.1 M Tris-HCl buffer containing 0.5 mM $MgCl_2$, pH 9.5. Assay conditions were optimized to ensure that color development was linear with respect to the quantity of microsomal protein or standard loaded and the time of the phosphatase reaction. The staining intensities of the protein bands were measured with a pdi 420oe densitometer (PDI, New York, USA) equipped with an AGFA Arcus II scanner (Agfa-Gevaert NV, Mortsel, Belgium) using the pdi Quantity One 3.0 software (Bio-Rad, Hercules, California, USA). The amount of immunoreactive protein was determined from the integrated intensity of the stained band to that of the internal standard and was expressed as relative optical density units per mg of microsomal protein. Liver microsomes prepared from individual mice were analyzed 2–4 times on different days.

Statistics. Nonparametric analyses of body and organ weights, body length and PCB congener levels were performed using Wilcoxon signed rank test for paired and unpaired comparisons using the litter as statistical unit as appropriate. Mean values were used for the statistical analysis when measurements from several littermates were available (see Supplementary Tables 1–8 for details regarding the number of animals). With exception of the qPCR results, all statistical procedures were performed using SAS software (SAS Institute, 2013). Differences between exposure groups were considered statistically different at $P < .05$. Analysis of the qPCR results was performed with SDS 2.4.1 (Thermo Scientific; version 2.4) and quantification of relative changes in transcript expression with REST 2009 software (Qiagen) using dams and 1 male and 1 female P21 pup from each litter. Statistical analysis was performed using REST 2009 (built-in randomization techniques) as previously described in Stamou *et al.* (2014).

RESULTS

General Toxicity and Reproductive Outcomes

Dietary exposure of female C57BL/6 mice to racemic PCB 95 or PCB 136 beginning 2 weeks prior to conception and continuing throughout gestation and lactation did not cause overt toxicity in dams (Supplementary Table 13). There were no significant differences in the growth curves (Supplementary Figure 1), final body weights or organ weights between PCB-exposed animals and vehicle control groups. Exposure of dams to PCB 95 and PCB 136 also did not alter reproductive outcomes or influence the body weights, body length and organ weights of pups at P3, P7, or P21 (Supplementary Tables 14 and 15). The only exceptions were a lower relative brain weight in male P7 pups exposed to PCB 136 and a larger kidney weight in female P21 pups exposed to PCB 95 compared with age-matched control pups.

Disposition of PCB 95 and Hydroxylated Metabolites

The levels of PCB 95 and 5 hydroxylated metabolites, designated as 3-103 (NIH shift product), 4-95, 4′-95, 5-95, and 4,5-95, were determined in tissues collected at the time points indicated in Figure 1. PCB 95 and these 5 hydroxylated metabolites were detected in all tissues investigated in this study. Additional PCB 95 metabolites may have been formed, but we were unable to detect and quantify these metabolites, in part due to the lack of authentic standards.

Whole body levels of PCB 95 and its OH-PCB metabolites in P3 and P7 pups. The whole body content of PCB 95 and its OH-PCB metabolites was determined in pups at P3 and P7. Whole body PCB 95 levels, adjusted for wet weight, decreased significantly between these time points from an average concentration of 3.6 nmol/g at P3 to 1.8 nmol/g at P7 (Figure 2A; Supplementary Table 1). This decrease in PCB 95 levels was accompanied by an increase in body weight of pups (Supplementary Table 14), suggesting that the increase in body weight resulted in a growth dilution of the internal PCB 95 dosage between P3 and P7. Consistent with this interpretation, the total amount of PCB 95 was comparable in P3 and P7 carcasses (Supplementary Figure 2A; Supplementary Table 5).

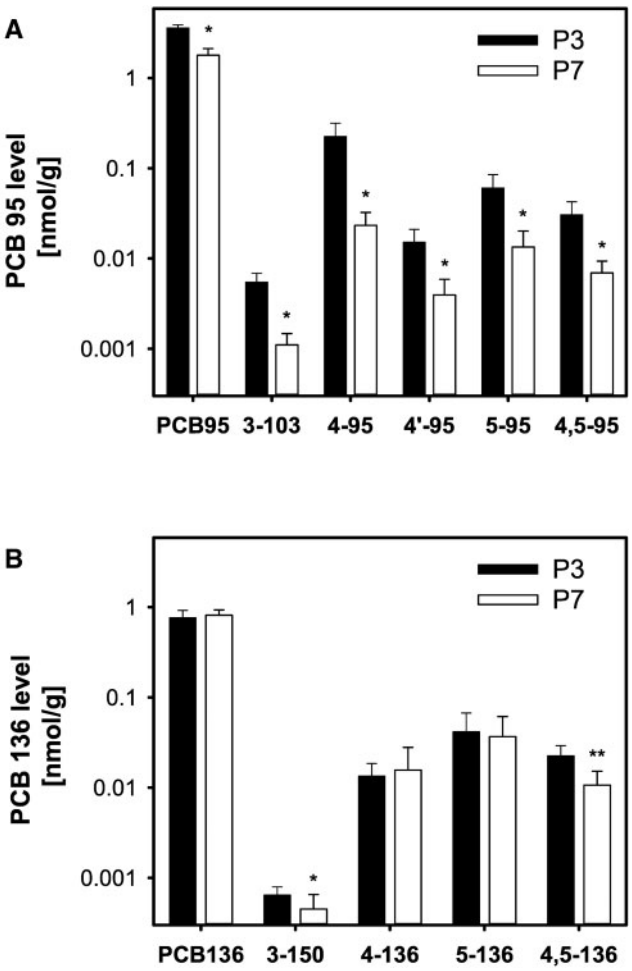

FIG. 2. Whole body levels of PCBs and their hydroxylated metabolites in P3 and P7 pups exposed to PCB 95 (A) or PCB 136 (B) in the maternal diet. For P7 pups, the carcass level is calculated as the sum of the brain level and level of the remaining carcass. Values are adjusted for tissue wet weight and presented on a logarithmic scale as mean ± SD of average levels for male and female pups from the same litter (n = 5 or 6 litters; see Supplementary Tables 1 and 2 for additional details). *Significantly different from P3 pups; $P < .05$. **Significantly different from P3 pups; $P < .01$.

The major metabolite of PCB 95 in carcasses at P3 and P7 was 4-95, followed by 5-95 > 4,5-95 > 4′-95 > 3-103 (Figure 2A). The wet weight adjusted levels of all 5 OH-PCB 95 metabolites as well as the sum of the 5 hydroxylated metabolites of PCB 95 quantified in this study ($\Sigma_{(5)}$OH-PCB 95) decreased significantly between P3 and P7. Growth dilution likely contributed to the lower PCB 95 metabolite levels; however, the total amount of all OH-PCB 95 metabolites decreased in carcasses from P3 to P7, with the decrease being statistically significant for 3-103, 4-95, and $\Sigma_{(5)}$OH-PCB 95 (Supplementary Figs. 2A and 3B; Supplementary Table S5). This comparison suggests that, in addition to growth dilution, other factors contributed to the lower OH-PCB 95 metabolite levels in P7 versus P3 carcasses. $\Sigma_{(5)}$OH-PCB 95 was 10- and 40-fold lower compared with PCB 95 levels in P3 and P7 carcasses, respectively (Figs. 3A and B; Supplementary Table 1).

Brain levels of PCB 95 and its OH-PCB metabolites in pups and dams. The mean level of PCB 95 in the brain of P7 pups was 0.15 nmol/g (Figure 3A; Supplementary Table 1), which corresponds to 2.4% of the total PCB 95 body burden. Moreover, PCB 95 levels in the brain were of a comparable magnitude in pups (0.15 and 0.21 nmol/g in P7 and P21 pups, respectively) and dams (0.14 nmol/g). The total amount of PCB 95 in the brain significantly increased from P7 to P21 (Supplementary Figure 3A; Supplementary Table 5) despite the near doubling of brain weight during this same time frame (Supplementary Tables 14 and 15).

The wet weight adjusted $\Sigma_{(5)}$OH-PCB 95 levels in the brain of P7 pups were 0.026 nmol/g (Figure 3B; Supplementary Table 1), which corresponds to 0.4% of the total body burden of $\Sigma_{(5)}$OH-PCB 95. $\Sigma_{(5)}$OH-PCB 95 levels were approximately 1 order of magnitude lower compared with PCB 95 levels at both P7 and P21 (Figs. 3A and B; Supplementary Table 1). $\Sigma_{(5)}$OH-PCB 95 levels decreased significantly from P7 to P21 both on a wet weight basis (Supplementary Table 1) and expressed as total amount in the whole brain (Supplementary Table 5), which suggests that this decrease is only partially due to growth dilution in the developing brain. $\Sigma_{(5)}$OH-PCB 95 levels in P21 pups and dams were comparable (0.010 and 0.007 nmol/g, respectively; Supplementary Table 1).

The metabolite profile in the brain of P7 pups differed from the profile found in their carcasses (Figs. 2A vs 4A), and from the metabolite profile found in the brain of P21 pups and their dams (Figure 4A; Supplementary Table 1). 4-95 and 4′-95, major metabolites formed in incubations with human liver microsomes (Uwimana *et al.*, 2016), were also the major metabolites in the brain of P7 pups, and their brain levels were comparable (0.008 and 0.007 nmol/g, respectively). 4,5-95, 3-103 and 5-95 were minor metabolites in the brain of P7 pups. In contrast, 4-95, 4′-95, and 5-95 were major metabolites in P21 pup brains, and 5-95 was the major metabolite in the brain of dams. These changes in the metabolite profiles in the brain were due to significant decreases in wet weight adjusted levels of 3-103, 4-95, 4′-95, and 4,5-95 from P7 to P21. The total amount of these 4 metabolites in the brain also decreased from P7 to P21; however, this decrease reached statistical significance only for 4,5-95 (Supplementary Table 5). At the same time, wet weight adjusted levels of 5-95 remained relatively constant in the brain at all 3 time points (0.0021–0.0023 nmol/g). No statistically significant differences in the wet weight adjusted levels or total amounts of OH-PCB 95 metabolites were observed in the brain from P21 pups versus the corresponding dams, with total amounts of 4′-95 being the only exception.

Tissue levels of PCB 95 and its OH-PCB metabolites in P21 pups. In addition to the brain, PCB levels were determined in blood, liver, and muscle of P21 pups (Figure 3A). The wet weight adjusted levels of PCB 95 were the highest in muscle, followed by liver > brain > blood (Supplementary Table 1).

Wet weight adjusted $\Sigma_{(5)}$OH-PCB 95 levels were comparable in liver, blood, and muscle from P21 pups (Figure 3B; Supplementary Table 1). The mean brain level of $\Sigma_{(5)}$OH-PCB 95 levels was approximately 10-fold lower than the levels observed in the other tissues. In blood, the levels of $\Sigma_{(5)}$OH-PCB 95 were similar to the level of PCB 95. In contrast, $\Sigma_{(5)}$OH-PCB 95 levels were approximately 4-fold lower than parent PCB 95 in liver and 60-fold lower in the muscle.

The OH-PCB metabolite profiles varied slightly between tissues, with the brain profile being different from the profile observed in all other tissues at P21 (Figure 5A). Specifically, 4-95 was the major OH-PCB 95 metabolite in blood and liver, with a rank order of 4-95 ≫ 4′-95 > 5-95 ≈ 4,5-95 ≈ 3-103. In contrast, levels of 4-95 and 4′-95 were comparable in the pup brain. 4′-95 was the major metabolite in the muscle, followed by 5-95 ≈ 3-103 > 4-95 > 4,5-95.

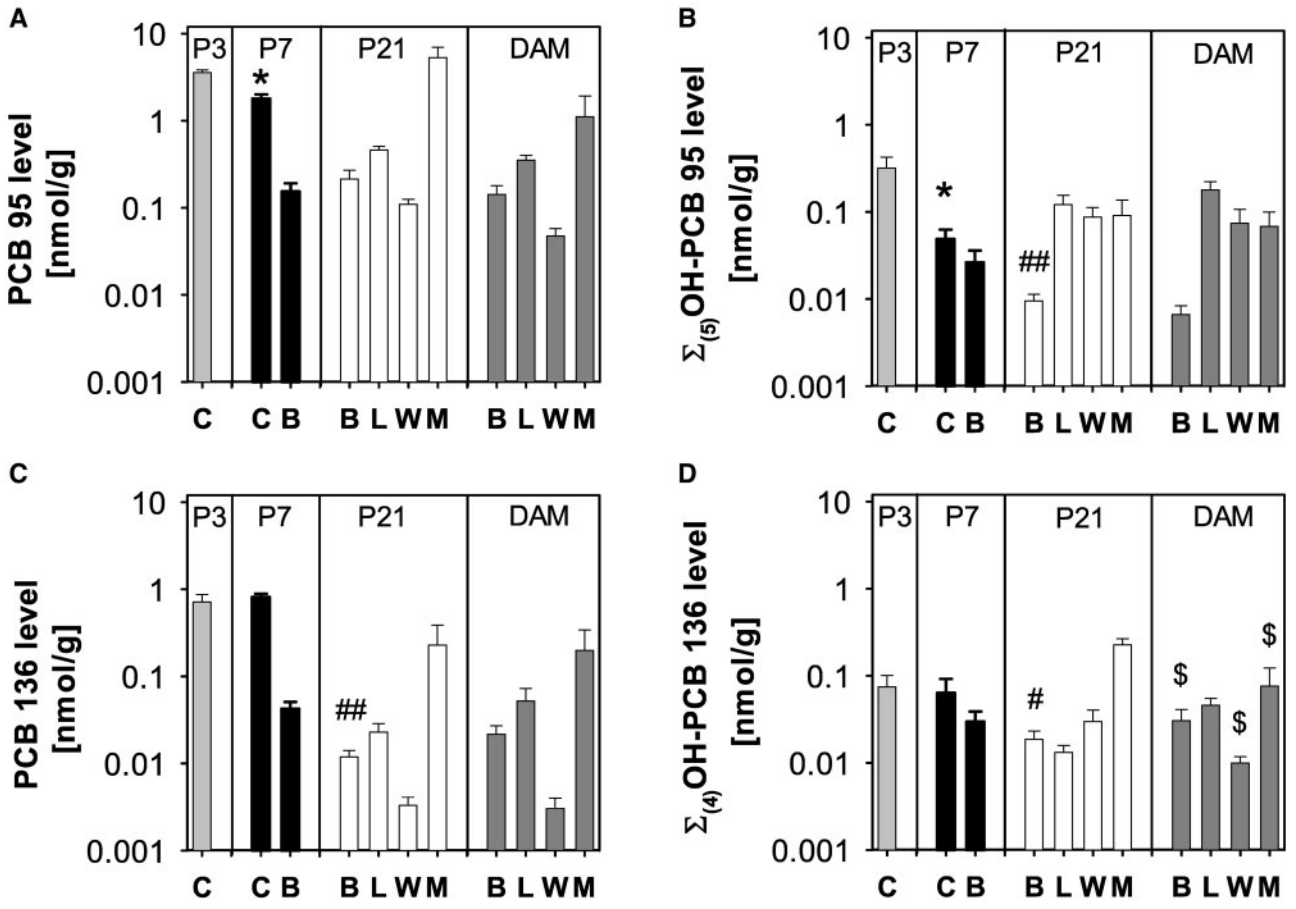

FIG. 3. Tissue levels of PCB 95 (A), $\Sigma_{(5)}$OH-PCB 95 (B), PCB 136 (C), and $\Sigma_{(4)}$OH-PCB 136 in (D) dams and the corresponding P3, P7, and P21 pups. Values are adjusted for tissue wet weight and presented on a logarithmic scale as mean ± SD of average levels for male and female pups from the same litter (n = 5 or 6 litters; see Supplementary Tables 1 and 2 for additional details). C, carcass; B, brain; L, liver; W, whole blood; M, muscle. *Significantly different from carcass of P3 pups; $P < .05$. # Significantly different from brain of P7 pups; $P < .05$; ## significantly different from brain of P7 pups; $P < .01$. $Significantly different from levels in the same tissue from pups euthanized on P21; $P < .05$.

Tissue levels of PCB 95 and its OH-PCB metabolites in dams. In dams, the highest wet weight adjusted level of PCB 95 was found in the muscle, followed by liver > brain > and blood (Figure 3A; Supplementary Table 1). No statistically significant differences were observed in the levels of PCB 95 in all tissues in dams versus P21 pups. However, because P21 pups have smaller livers compared with the respective dams (approximately 0.6 g vs 1.8 g, respectively; Supplementary Tables 13 and 15), total amounts of PCB 95 were significantly higher in the liver of dams compared with their P21 pups (Supplementary Figs. 3A; Supplementary Table 5).

In dams, the highest wet weight adjusted levels of $\Sigma_{(5)}$OH-PCB 95 were present in the liver, followed by blood ≈ muscle ≫ brain (Figure 3B; Supplementary Table 1). When compared with levels of parent PCB 95, $\Sigma_{(5)}$OH-PCB 95 levels were lower in the brain, liver and muscle, but slightly higher in blood than PCB 95 levels (Supplementary Table 1). The major metabolite in all tissues and blood was 4-95, but the metabolite profiles varied between tissues, with a different profile observed in brain compared with the profiles observed in the other tissues (Figure 6A). Metabolite profiles observed in tissues from dams and their P21 pups displayed similar features, in particular the liver and blood (Figs. 6A vs 5A). As with the parent PCB, total amounts of all OH-PCB 95 metabolites in the liver were significantly higher in dams compared with their P21 pups due to the differences in liver size (Supplementary Figure 5A; Supplementary Table 5).

Disposition of PCB 136 and Hydroxylated Metabolites

The levels of PCB 136 and 4 hydroxylated metabolites, including 3-150 (NIH shift product), 4-136, 5-136, and 4,5-136, were determined at the time points and the tissues identified in Figure 1. PCB 136 and all 4 hydroxylated metabolites were detected in all tissues analyzed in this study. Additional metabolites of PCB 136 may have been formed, but could not be detected because of the lack of authentic standards.

Whole body levels of PCB 136 and its OH-PCB metabolites in P3 and P7 pups. The wet weight adjusted levels of PCB 136 were comparable in the carcass of pups at P3 and P7 (0.71 and 0.81 nmol/g, respectively) (Figure 2B; Supplementary Table 2). The levels of PCB 136 were 5- and 2-fold lower than levels of PCB 95 in the whole body of P3 and P7 pups, respectively (Figs. 2 vs 3; Supplementary Tables 2 vs 1). Unlike PCB 95, the total amount of PCB 136 in the carcass significantly increased from P3 to P7, despite the considerable growth of the pups (Supplementary Figure 2B; Supplementary Table 6).

The major metabolite of PCB 136 in P3 and P7 carcasses was 5-136 followed by 4,5-136 ≈ 4-136 (Figure 2B). The NIH shift metabolite 3-150 was found only in trace amounts at both time points. The wet weight adjusted levels of 3-150 and 4,5-136, but not the other metabolites, decreased significantly between P3 and P7. Because total amounts of the OH-PCB 136 metabolites in the carcass do not significantly change (Supplementary Figure 2B;

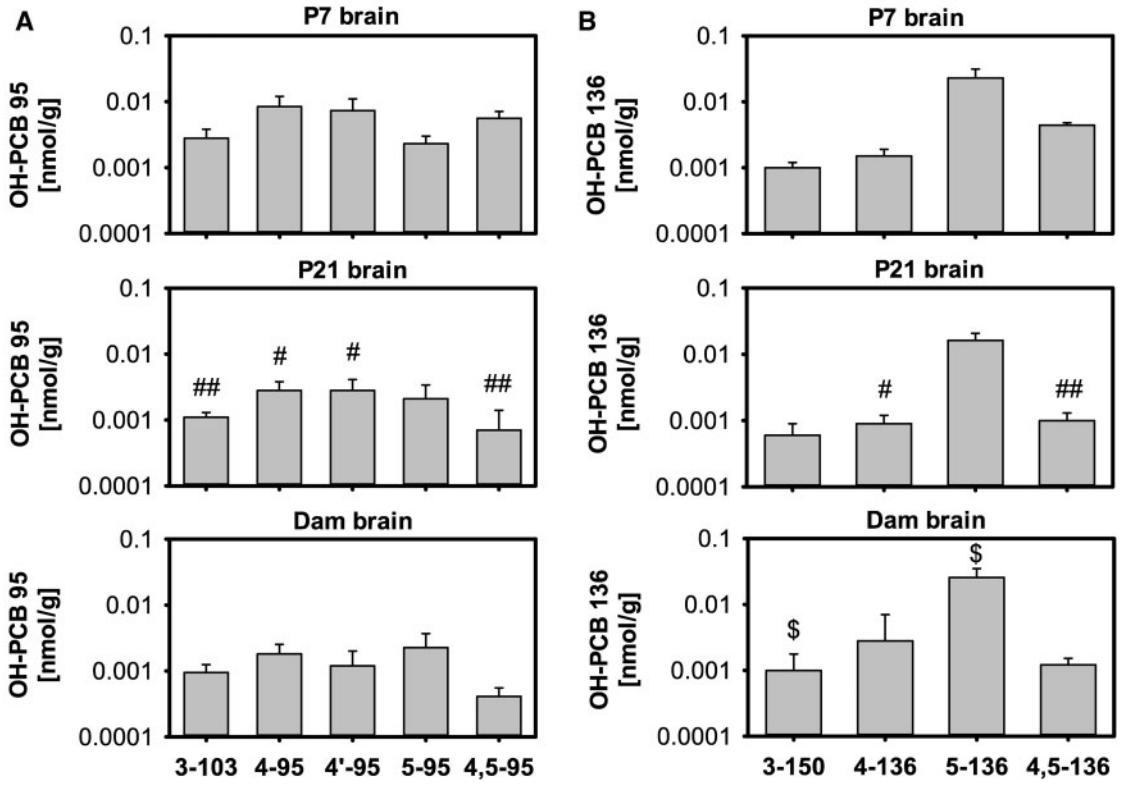

FIG. 4. Brain profiles of OH-PCB metabolites differ among P7 and P21 pups and dams exposed to PCB 95 (A) or PCB 136 (B). Values are adjusted for tissue wet weight and presented on a logarithmic scale as mean ± SD of average levels for male and female pups from the same litter (n = 5 or 6 litters; see Supplementary Tables 1 and 2 for additional details). #OH-PCB levels significantly different from brain of P7 pups; $P < .05$; ## OH-PCB levels significantly different from brain of P7 pups; $P < .01$. $OH-PCB levels significantly different from levels in the same tissue from pups euthanized on P21; $P < .05$.

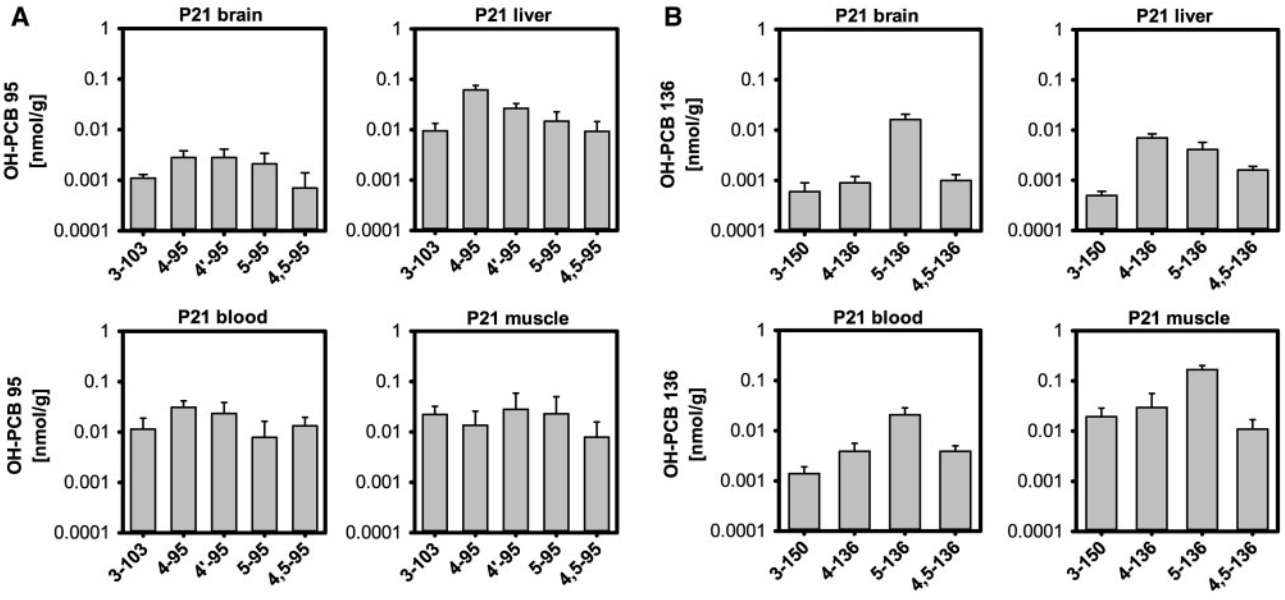

FIG. 5. Tissue profiles of OH-PCB metabolites in P21 pups from PCB 95-exposed dams (A) or PCB 136-exposed dams (B). Values are adjusted for tissue wet weight and presented on a logarithmic scale as mean ± SD of average levels for male and female pups from the same litter (n = 5 or 6 litters; see Supplementary Tables 1 and 2 for additional details).

Supplementary Table 6), the decrease in wet weight adjusted 3-150 and 4,5-136 levels is, at least in part, due to growth dilution from P3 to P7 (Supplementary Figure 1B; Supplementary Table 6). The sum of the 4 hydroxylated metabolites ($\Sigma_{(4)}$OH-PCB 136) in the whole body of P3 and P7 pups was approximately 10-fold lower than the parent PCB 136 levels, and did not change significantly from P3 to P7 (Figs. 3C and D; Supplementary Table 2). The levels of $\Sigma_{(4)}$OH-PCB 136 were approximately 4-times lower

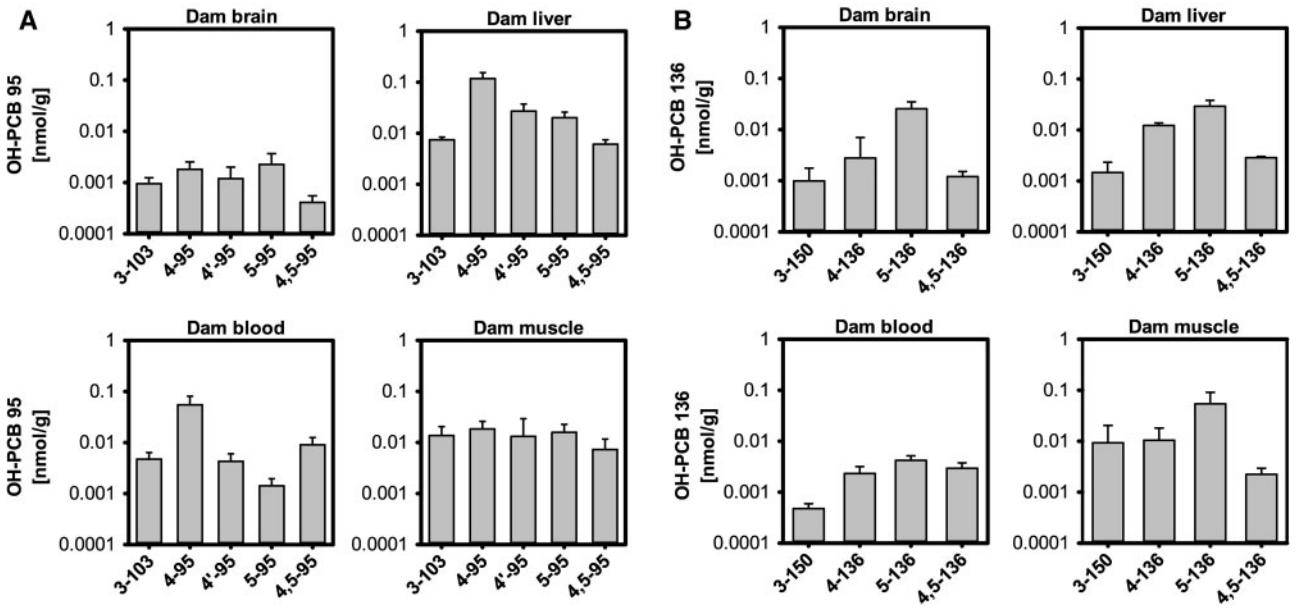

FIG. 6. Tissue profiles of OH-PCB metabolites in PCB 95- (A) or PCB 136-exposed dams (B). Values are adjusted for tissue wet weight and presented on a logarithmic scale as mean ± SD; see Supplementary Tables 1 and 2 for additional details.

than levels of $\Sigma_{(5)}$OH-PCB 95 at P3, but comparable on P7 (Figs. 3B vs D).

Brain levels of PCB 136 and its OH-PCB metabolites in pups and dams. Wet weight adjusted PCB 136 levels in the brain of P7 pups (0.043 nmol/g) corresponded to approximately 0.2% of the total PCB 136 body burden and significantly decreased from P7 to P21 (Figure 3C; Supplementary Table 2). A significant decrease in the total amount of PCB 136 in the brain was also observed from P3 to P7 (Supplementary Figure 3C; Supplementary Table 6). Together, these observations suggest that, in addition to growth dilution, other factors contribute to changes in the levels of PCB 136 in the developing brain. Moreover, the levels of PCB 136 in the brain of pups and dams were lower than levels of PCB 95 (Figs. 3A vs D; Supplementary Figs. 3A vs C).

The wet weight adjusted $\Sigma_{(4)}$OH-PCB 136 levels in the brain of pups at P7 were 0.030 nmol/g (Figure 3D; Supplementary Table 2), which corresponds to 2.6% of the total body burden of $\Sigma_{(4)}$OH-PCB 136. Brain levels of $\Sigma_{(4)}$OH-PCB 136 varied significantly between P7 and P21 pups, with significantly lower levels (0.019 nmol/g) being observed in the brain of P21 pups (Figure 3D; Supplementary Table 2). Wet weight adjusted levels of all 4 OH-PCB 136 metabolites decreased from P7 to P21, with changes being significant for 4-136 and 4,5-136 (Figure 4B; Supplementary Table 2). This decrease in OH-PCB 136 levels is due to growth dilution because the total amounts of $\Sigma_{(4)}$OH-PCB 136 in the brain of P7 and P21 pups were comparable (Supplementary Figure 3D; Supplementary Table 6). 4,5-136 was an exception, because, similar to 4,5-95, the total amount of this metabolite in the brain decreased significantly from P7 to P21 (Supplementary Figure 4B). Importantly, wet weight adjusted $\Sigma_{(4)}$OH-PCB 136 levels in the brain of P7 and P21 pups and dams were of the same order of magnitude as levels of PCB 136. When compared with PCB 95-exposed pups, $\Sigma_{(4)}$OH-PCB 136 levels were similar to $\Sigma_{(5)}$OH-PCB 95 levels in the brain of P7 pups, but 2-fold higher in P21 pups (Figure 3; Supplementary Table 1).

The metabolite profile in the brain of P7 pups, expressed on a wet weight basis, differed slightly from the profile found in carcasses due to slightly higher levels of 3-150, the NIH-shift product, in the brain compared with the carcass (Figs. 2B vs 4B). Differences were also noted in the OH-PCB profiles in the brain of P21 pups and their dams compared with P7 pups (Figure 4B). Overall, 5-136 was the major metabolite in the brain of P7 and P21 pups and dams. However, levels of the catechol metabolite 4,5-136 were higher than 4-136 levels in the brain of P7 pups whereas levels of both metabolites were comparable in the brain of P21 pups, and 4-136 levels were higher than 4,5-136 levels in dams. The NIH shift metabolite 3-150 was a minor metabolite at all time points investigated.

Tissue levels of PCB 136 and its OH-PCB metabolites in P21 pups. The wet weight adjusted levels of PCB 136 were the highest in muscle, followed by liver > brain > blood (Figure 3C; Supplementary Table 2). PCB 136 tissue levels were much lower than levels of PCB 95 in the P21 pups (Supplementary Tables 2 vs 1 and 6 vs 5).

The wet weight adjusted $\Sigma_{(4)}$OH-PCB 136 levels in the tissues investigated followed the rank order: muscle $\gg$ blood > brain $\approx$ liver (Figure 3D; Supplementary Table 2). Levels of $\Sigma_{(4)}$OH-PCB 136 and PCB 136 were comparable in the brain and muscle, whereas $\Sigma_{(4)}$OH-PCB 136 blood levels were approximately 1 order of magnitude higher than PCB 136 levels. In contrast, $\Sigma_{(4)}$OH-PCB 136 liver levels were almost 2 times lower compared with levels of PCB 136. $\Sigma_{(4)}$OH-PCB 136 levels were lower than $\Sigma_{(5)}$OH-PCB 95 levels in the liver and blood, but higher in brain and muscle in P21 pups (Figs. 3B vs D; Supplementary Tables 1 vs 2).

The OH-PCB 136 metabolite profiles in P21 pups varied between tissues (Figure 5B). With exception of the liver, 5-136 was the major metabolite in all tissues investigated. The rank order of OH-PCB metabolites was 5-136 $\gg$ 4,5-136 $\approx$ 4-136 > 3-150 in blood and brain and 5-136 $\gg$ 4-136 > 3-150 > 4,5-136 in muscle. In contrast, 4-136 was major metabolite in the liver, followed by 5-136 > 4,5-136 > 3-150.

Tissue levels of PCB 136 and its OH-PCB metabolites in dams at P21. The highest wet weight adjusted levels of PCB 136 in dams were

found in the muscle followed by liver, brain and blood (Figure 3C; Supplementary Table 2). The same rank order was observed in P21 pups from the PCB 136 exposure group, and PCB 136 levels in tissues from dams were comparable to levels found in P21 pups. When expressed as the total amount per organ, PCB 136 levels in the liver were significantly higher in dams compared with P21 pups due to the larger size of the liver in dams (Supplementary Figure 3C; Supplementary Table 6). PCB 136 levels were lower in all tissues compared with PCB 95-exposed dams (Supplementary Tables 2 vs 1 and 6 vs 5).

In dams, the highest $\Sigma_{(4)}$OH-PCB 136 levels, adjusted for wet weight, were detected in the muscle, followed by the liver ≈ brain > blood (Figure 3D; Supplementary Table 2). $\Sigma_{(4)}$OH-PCB 136 levels were lower in muscle, but higher in blood compared with PCB 136 levels. In contrast, levels of PCB 136 and $\Sigma_{(4)}$OH-PCB 136 were similar in brain and liver. As observed with the OH-PCB 95 metabolites discussed earlier, total amounts of all OH-PCB 136 metabolites in the liver were significantly higher in dams compared with their P21 pups due to the differences in liver size (Supplementary Figures 6B vs 5B; Supplementary Table 6). Comparison of the 2 PCB exposure groups revealed similar levels of $\Sigma_{(4)}$OH-PCB 136 and $\Sigma_{(5)}$OH-PCB 95 in muscle, but higher $\Sigma_{(4)}$OH-PCB 136 levels in the other tissues, including the brain (Figs. 3B vs D; Supplementary Tables 2 vs 1).

Similar profiles of OH-PCBs were observed in brain and liver from dams, with metabolite levels decreasing in the order 5-136 > 4-136 > 4,5-136 > 3-150 (Figure 6B). The rank order in the blood (5-136 > 4,5-136 ≈ 4-136 > 3-150) and muscle (5-136 > 4-136 ≈ 3-154 > 4,5-136) was slightly different from the profiles observed in brain and liver. As in the PCB 95 exposure group, OH-PCB 136 tissue profiles of P21 pups and the corresponding dams displayed similar features (Figs. 6B vs 5B). The liver was an exception because 5-136 and not 4-136, was the major metabolite in dams.

Enantiomeric Enrichment of PCB 95

The enantiomeric enrichment of PCB 95 was determined using enantioselective gas chromatography (Supplementary Table 9). The second eluting atropisomer of PCB 95, designated as E_2-PCB 95, was enriched in all tissues from pups and dams. The direction and extent of enantiomeric enrichment was similar in carcasses from P3 and P7 pups (EF of 0.12 and 0.17, respectively). Enantiomeric enrichment of E_2-PCB 95 in the brain of P7 pups appeared to be more pronounced than in the carcass (EF of 0.07 vs 0.17, respectively). Enantiomeric enrichment of E_2-PCB 95 was comparable in the brains of P7 and P21 pups and the dams, with EF values ranging from 0.05 to 0.07. The most pronounced enantiomeric enrichment was observed in the liver and brain of P21 pups, followed by blood and muscle. In dams, the extent of the enantiomeric enrichment decreased in the order brain > blood ≈ liver > muscle. In previous studies with adult female mice exposed to PCB 95, the liver exhibited the most pronounced enantiomeric enrichment, with the rank order liver > brain ≥ blood (Kania-Korwel *et al.*, 2012, 2015). It is noteworthy that the enrichment of E_2-PCB 95 in the muscle was less pronounced in dams than in P21 pups (EF of 0.27 vs 0.11, respectively).

Enantiomeric enrichment of a single PCB 95 metabolite, 4-95, was determined in the carcasses of P3 and P7 pups, liver of P21 pups and blood and liver from the dams (Supplementary Table 9). The atropisomer of 4-95 eluting second on the chiral column, designated as E_2-4-95, was enriched in all tissues analyzed. EF values of 4-95 typically ranged from 0.11 to 0.14, except for livers from dams, which displayed less pronounced enrichment (EF = 0.22).

Enantiomeric Enrichment of PCB 136

Enantioselective gas chromatography revealed an enrichment of the PCB 136 atropisomer eluting second on the chiral column (E_2-PCB 136) in all tissues under investigation (Supplementary Table 9). Enantiomeric enrichment of PCB 136 in carcasses from P3 and P7 pups was similar, with EF values of 0.21 and 0.25, respectively. Moreover, enantiomeric enrichment in the brain and carcasses from P7 pups was comparable, with EF values of 0.28 and 0.25, respectively. A slight increase in the extent of enantiomeric enrichment from P7 to P21 was noted in the brain (EF = 0.28 vs 0.21). The most pronounced enantiomeric enrichment was observed in the liver of P21 pups, followed by brain and muscle. In dams, the extent of the enantiomeric enrichment decreased in the order liver > blood ≈ muscle. Furthermore, PCB 136 residues in liver and muscle displayed less pronounced enantiomeric enrichment in dams compared with the corresponding P21 pups. When compared with the PCB 95 exposure group, less pronounced enantiomeric enrichment was observed in pups and dams from the PCB 136 exposure group. Moreover, changes in chiral PCB signatures in several compartments, such as the brain, differed slightly between PCB 95 and PCB 136 exposure groups.

Effect of PCB Exposure on Hepatic Expression of P450 Enzymes

Transcript levels of hepatic P450 enzymes in P21 pups and dams. Hepatic *cyp1a2*, *cyp2b10*, and *cyp3a11* mRNA levels were quantified using qPCR (Table 1) to allow a comparison with our earlier study investigating the expression of these enzymes in liver and different brain regions (Stamou *et al.*, 2014). The overall effects of PCB exposure on P450 gene expression in the liver of P21 pups and their dams were modest. The most intriguing observation was a significant increase in *cyp2b10* transcript levels in male pups from the PCB 95 exposure group compared with age- and sex-matched control pups. PCB 95 exposure had no other effect on P450 gene expression in the liver. The expression of *cyp1a2* was significantly decreased in female pups from the PCB 136 exposure group compared with control pups. Additionally, transcript levels of *cyp3a11* were significantly lower in dams from the PCB 136 exposure group compared with control dams.

Protein levels of P450 enzymes in P21 pups and dams. Relative hepatic protein levels of selected P450 enzymes were determined in P21 pups and their dams to assess whether the effect of PCB exposure on P450 gene expression translated to changes at the protein level (Table 2). Antibodies specific for Cyp1a, Cyp2b and Cyp3a allowed the detection and quantification of several mouse P450 isoforms, which were tentatively identified as mouse Cyp1a2, Cyp2b9 (upper band), Cyp2b10 (lower band), Cyp3a11 (upper band), Cyp3a41 (middle band), and Cyp3a13/25 (lower band), respectively. Protein levels of Cyp2b10, Cyp2b9, and Cyp3a13/25 were lower and the protein level of Cyp3a11 was higher in pups from the control group compared with their dams, but these differences did not reach statistical significance. Cyp3a41 was not detected in the liver of pups from any exposure group, but was expressed in dams from all 3 exposure groups.

PCB 95 exposure significantly increased Cyp2b10 protein levels in the liver of both female and male pups compared with age and sex-matched control pups. This observation is consistent with the significant increase in *cyp2b10* transcript levels in male

Table 1. Changes in P450 Gene Expression in Livers of Dams Exposed to PCB 95 or PCB 136 and Their Female and Male P21 Pups Shown Relative to Age and Sex-Matched Control Animals

PCB Exposure		*cyp1a2*		*cyp2b10*		*cyp3a11*	
		Relative expression	95% CI	Relative expression	95% CI	Relative expression	95% CI
PCB 95	Female pups	0.55	0.10–2.5	1.0	0.37–4.0	0.63	0.16–2.0
	Male pups	0.77	0.16–2.9	**3.3*a*↑ (*P* = .01)**	0.81–8.6	1.1	0.35–3.3
	Dams	0.57	0.11–1.7	0.74	0.17–4.2	0.74	0.20–2.9
PCB 136	Female pups	**0.52*a*↓ (*P* = .004)**	0.27–0.95	1.6	0.29–8.6	0.80	0.45–1.4
	Male pups	0.86	0.23–2.8	2.0	0.28–6.3	1.0	0.33–2.3
	Dams	0.65	0.20–1.8	1.0	0.37–3.1	**0.47*a*↓ (*P* = .02)**	0.21–1.4

[a]Indicates statistically significant change (↑: upregulation; ↓: downregulation) of gene expression ($P < .05$). The relative expression (shown in bold) is calculated as described before in Stamou et al. (2014, 2015), followed by the *P*-value in parentheses. Gene transcript levels were normalized against the mean transcript level of *pgk1* as the reference gene. Relative expression, *P*-values and 95% CIs were calculated using the REST2009 software (Qiagen), which incorporates Ct and efficiency values determined by qPCR analysis.

pups from the PCB 95 exposure group compared with control pups. With exception of a slight, but statistically significant decrease in Cyp3a11 protein levels, no significant differences in the protein levels of any P450 isoform investigated were observed in PCB 95-exposed dams compared with control dams. Protein levels of Cyp2b10 were lower and protein levels of Cyp1a2 and Cyp3a11 were higher in female and male pups from the PCB 95-exposed group compared with their dams; however, these differences did not reach statistical significance.

PCB 136 exposure significantly increased hepatic Cyp1a2 protein in male pups, increased Cyp2b10 protein levels in both female and male pups, and increased Cyp2b9 is female pups relative to the respective control pups. Moreover, protein levels of Cyp2b10 and all 3 Cyp3a enzymes were significantly lower in the liver of PCB 136-exposed dams compared with control dams. Consistent with this finding, transcript levels of *cyp3a11* were lower in dams from the PCB 136 exposure group compared with control dams. Cyp2b10 protein levels were lower and Cyp3a11 protein levels were higher in both female and male pups from the PCB 136-exposed group compared with their dams. Cyp1a2 protein levels were also higher in pups compared with their dams; however, this difference reached statistical significance only for male pups in the PCB 136 exposure group.

Effect of PCB Exposure on Expression of Neural Plasticity and Thyroid Hormone-Responsive Genes in Brains of P21 Pups

As an initial screen of the potential developmental neurotoxicity of PCB 95 and PCB 136, transcript levels of genes encoding proteins involved in activity-dependent neural plasticity as well as thyroid hormone-responsive genes were quantified in the cortex, hippocampus and cerebellum of P21 pups by qPCR. Neural plasticity genes included *arc*, which encodes activity-regulated cytoskeleton-associated protein, and *ppp1r9b*, which encodes protein phosphatase 1 regulatory subunit 9B, also known as spinophilin or neurabin-II; thyroid hormone-responsive genes included *nrgn*, which encodes RC3/neurogranin, and *mbp*, which encodes myelin basic protein (Table 3). These genes were selected because *arc* (Kim and Huganir, 1999; Segal, 2001), *nrgn* (Krucker *et al.*, 2002), and *ppp1r9b* (Kim and Huganir, 1999; Segal, 2001) are potential biomarkers of synapse density and synaptic plasticity; *nrgn* and *mbp* are thyroid hormone-responsive genes whose expression have been previously shown to be altered by PCBs (Zoeller *et al.*, 2000).

Developmental exposure to PCB 95 decreased expression of thyroid hormone-responsive genes in a sex-, brain region-, and transcript-specific manner. For example, relative to age-, sex-, and brain region-matched controls, *mbp* expression was significantly lower in the cerebellum of PCB 95-exposed female but not male pups, while *nrgn* transcript levels were significantly decreased in the hippocampus of both female and male pups (Table 3). However, PCB 95 exposure had no significant effect on expression of the neural plasticity genes *arc* or *ppp1r9b* in any brain region.

Developmental exposure to PCB 136 affected the expression of both neural plasticity and thyroid hormone-responsive genes in P21 pups compared with age- and sex-matched control animals (Table 3). Expression of the neural plasticity gene *ppp1r9b* was significantly elevated in the cortex of PCB 136-exposed male and female pups, and in the hippocampus of PCB 136-exposed male pups. In contrast, transcript levels of the neural plasticity gene *arc* were significantly decreased in the cerebellum and significantly increased in the cortex of female pups exposed to PCB 136. Exposure to PCB 136 altered expression of thyroid hormone-responsive genes, *mpb* and *nrgn*, in the cerebellum and hippocampus but not the cortex. In the cerebellum, *mbp* transcripts were significantly decreased in PCB 136-exposed female and male pups. Expression of *nrgn* was significantly lower in the hippocampus, but significantly higher in the cerebellum of female pups exposed to PCB 136.

DISCUSSION

Chiral PCBs are major constituents of technical PCBs mixtures, and significant amounts of these PCB congeners have been released into the environment (Kania-Korwel and Lehmler, 2016a). Laboratory and human studies implicate exposure to these PCB congeners, in particular PCB 95 and PCB 136, in PCB-mediated developmental neurotoxicity, most likely by mechanisms involving RyRs (Bal-Price *et al.*, 2017; Lesiak *et al.*, 2014; Mitchell *et al.*, 2012; Pessah *et al.*, 2006; Wayman *et al.*, 2012a,b; Yang *et al.*, 2014). However, limited information is available regarding the enantioselective disposition of RyR-active PCBs and their metabolites in lactating mice and their offspring. To close this knowledge gap, this study investigated the levels and chiral signatures of PCB 95 and PCB 136 and their hydroxylated metabolites in dams and pups following dietary exposure of the dams to equimolar doses of the racemic parent compound. Additionally, congener-specific changes in the expression of hepatic P450 enzymes as well as brain levels of transcripts of neural plasticity and thyroid hormone-responsive genes were assessed.

Table 2. Relative P450 Protein Levels in Hepatic Microsomes Prepared From Dams Exposed to PCB 95 or PCB 136 and Their P21 Pups (Relative OD/mg Microsomal Protein)[a, b]

Group	Cyp1a2		Cyp2b				Cyp3a					
			Cyp2b10		Cyp2b9		Cyp3a11		Cyp3a41		Cyp3a13/25	
			Upper band		Lower band		Upper band		Middle band		Lower band	
	Female	Male	Female	Male	Female	Male	Female	Male	Female	Male	Female	Male
PUPS												
Vehicle ($n♀ = 4$, $n♂ = 4$)	76 ± 13	63 ± 10	5.7 ± 1.3$^{\#}$	3.1 ± 1.1	11 ± 2$^{\#}$	7 ± 2	12 ± 3	11 ± 2	ND	ND	3.2 ± 0.8	2.9 ± 0.6
PCB 95 ($n♀ = 5$, $n♂ = 5$)	75 ± 25	82 ± 21	9.4 ± 3.2*	7.1 ± 2.1*	13 ± 5	10 ± 3	11 ± 4	12 ± 5	ND	ND	3.5 ± 1.4	3.6 ± 1.7
PCB 136 ($n♀ = 6$, $n♂ = 6$)	84 ± 13	93 ± 7$^{*\$}$	8.9 ± 2.0$^{*\$}$	6.6 ± 2.4$^{*\$}$	17 ± 3$^{\#\#}$	12 ± 3	15 ± 3$^{\$}$	14 ± 2$^{\$}$	ND	ND	3.4 ± 1.2	2.9 ± 0.6
DAMS												
Vehicle (n = 5)		69 ± 15		23 ± 5		17 ± 3		6.7 ± 0.1		16 ± 1		6.6 ± 1.1
PCB 95 (n = 5)		62 ± 3		21 ± 2		14 ± 1		5.5 ± 0.9*		14 ± 2		5.4 ± 0.9
PCB 136 (n = 6)		64 ± 17		18 ± 3*		14 ± 3		3.6 ± 1.1**		13 ± 1**		4.6 ± 0.9*

[a]Relative OD is defined as the optical density (ie, contour quantity) of the P450 immunoreactive band/optical density of the internal standard band. Representative immunoblots are shown in Supplementary Figs. 7-9.
[b]One female and one male pup from each litter were analyzed. Values are presented as mean ± SD. ND, not detected.
Significantly different from the corresponding pups or dams from the control group, $^{*}P < .05$; $^{**}P < .01$,
Significantly different from their respective dams, $^{\$}P < .05$.
Significantly different from the corresponding male pups in the same exposure group, $^{\#}P < .05$.

Developmental exposure via the maternal diet resulted in the transfer of PCBs from the dam to the pups. For the time points investigated, growth dilution was a factor contributing to decreasing levels of both PCB congeners and their metabolites as pups aged. However, growth dilution could not explain all the age-related difference, suggesting that other factors, such as age-dependent changes in the expression of drug metabolizing enzymes or the composition of tissue compartments, also influenced the disposition of both PCB congeners. The disposition of PCB 95 and PCB 136 in dams and pups differed markedly from each other, with PCB 95 levels being approximately 1 order of magnitude higher than PCB 136 levels at comparable time points. The blood level of PCB 95 in dams, which was 16 ng/g, is comparable to the blood level (14 ng/g) reported in an earlier disposition study of PCB 95 in mice (Kania-Korwel *et al.*, 2015). Similar mean blood levels of PCB 95 were observed in studies of occupationally exposed workers (Wingfors *et al.*, 2006; Wolff *et al.*, 1992). The levels of PCB 95 in brains from pups and dams observed in our study were higher than levels of PCB 95 reported in postmortem human brain samples (Mitchell *et al.*, 2012). A biomonitoring study in women of reproductive age in the United States reported PCB 136 blood levels ranging from 0.54 to 22.3 ng/g (Whitcomb *et al.*, 2005), which is comparable to the blood levels of PCB 136 (1.1 ng/g) observed in dams in our study. These comparisons demonstrate that the PCB dosage employed in our study results in blood and tissue concentrations that reflect levels of these congeners in some human populations.

The higher tissue levels of PCB 95 compared with PCB 136 in lactating mice and their offspring in this study are consistent with a previous study that demonstrated P450 enzyme-mediated formation of OH-PCBs in mouse liver is more rapid for PCB 136 than PCB 95 (Wu *et al.*, 2013). In addition, congener-specific modulation of hepatic P450 enzyme activity following exposure to PCB 95 versus PCB 136 likely contributes to the observed differences in the disposition of these congeners in lactating mice and their offspring. Indeed, we observed small, but statistically significant effects of PCB exposure on the expression of hepatic P450 enzymes at the transcript and protein levels. The observation that dietary PCB exposure of the dams differentially increased the expression of hepatic Cyp2b enzymes in the pups is of particular interest because these P450 isoforms metabolize both PCB congeners in mammals (Lu *et al.*, 2013; Waller *et al.*, 1999; Warner *et al.*, 2009). We also noted several effects on the expression of hepatic Cyp3a enzymes, possibly due to cross-talk between CAR and PXR (Yang and Wang, 2014). These findings suggest that chiral PCBs and their metabolites modulate their own enantioselective metabolism, which in turn may influence their developmental neurotoxicity in the mouse. It is likely that both PCB congeners and their metabolite also differentially alter the expression of other drug metabolizing enzymes in the mouse.

Hepatic metabolism by P450 enzymes, in particular Cyp2b enzymes (Lu *et al.*, 2013; Waller *et al.*, 1999; Warner *et al.*, 2009), in the dam and pups results in significant enantiomeric enrichment of the PCB 95 and PCB 136 atropisomer eluting second on the chiral column (*i.e.*, E_2-PCB 95 and E_2-PCB 136). The observation that the levels and EF values of PCB 95 and PCB 136 differ in dams and nursing offspring has implications for interpreting the developmental neurotoxic potential of both PCB congeners in mice. In particular, RyR activation has been proposed as a convergent mechanism of PCB developmental neurotoxicity (Bal-Price *et al.*, 2017; Pessah *et al.*, 2010) and is implicated in the developmental neurotoxicity of PCB 95 and PCB 136 (Lesiak *et al.*, 2014; Wayman *et al.*, 2012a,b; Yang *et al.*, 2009). Indeed,

Table 3. Changes in Expression of Neural Plasticity and Thyroid Hormone-Responsive Genes in the Cerebellum, Cortex, and Hippocampus From P21 Pups of Dams Exposed to PCB 95 or PCB 136, Relative to Age- and Sex-Matched Vehicle Control Animals

Comparison			*arc*		*mbp*		*nrgn*		*ppp1r9b*	
			Relative expression	95% CI	Relative expression	95% CI	Relative expression	95% CI	Relative expression	95% CI
PCB 95	Cb	Female	1.4	0.59–7.5	**0.60*a* ↓ (*P* = .003)**	0.15–1.0	3.4	0.65–158	1.2	0.19–4.4
		Male	0.67	0.37–1.2	0.61	0.31–1.1	0.78	0.16–4.9	1.1	0.59–4.0
	Ctx	Female	2.0	0.11–17	0.42	0.07–1.8	1.1	0.01–19	0.99	0.08–6.7
		Male	2.0	0.51–17	0.58	0.17–1.6	1.3	0.35–34	1.3	0.23–13
	Hippo	Female	0.62	0.24–1.5	0.82	0.26–2.1	**0.70*a* ↓ (*P* = .006)**	0.53–0.94	0.70	0.12–3.5
		Male	1.3	0.53–2.8	1.1	0.32–2.7	**0.79*a* ↓ (*P* = .006)**	0.60–1.0	1.9	0.35–7.4
PCB 136	Cb	Female	**0.56*a* ↓ (*P* = .03)**	0.29–1.5	**0.57*a* ↓ (*P* = .02)**	0.33–1.2	**2.1*a* ↑ (*P* = .02)**	0.93–5.9	1.3	0.27–4.2
		Male	0.69	0.36–1.5	**0.67*a* ↓ (*P* = .05)**	0.37–1.4	0.39	0.06–2.8	1.3	0.55–5.1
	Ctx	Female	**2.9*a* ↑ (*P* = .04)**	0.59–21	0.7	0.33–1.6	2.7	0.61–20	**3.8*a* ↑ (*P* = .006)**	0.98–12
		Male	1.2	0.15–13	1.3	0.49–2.8	1.0	0.21–28	**2.0*a* ↑ (*P* = .04)**	0.82–12
	Hippo	Female	0.83	0.35–2.1	1.0	0.49–2.0	**0.80*a* ↓ (*P* = .02)**	0.60–1.1	1.1	0.52–3.1
		Male	1.2	0.43–2.6	1.6	0.61–3.6	0.85	0.62–1.2	**2.6*a* ↑ (*P* = .05)**	0.43–9.3

[a]Indicates statistically significant change (↑: upregulation; ↓: downregulation) of gene expression ($P < .05$). The relative expression (shown in bold) is calculated as described before in Stamou et al. (2014, 2015), followed by the *P*-value in parentheses. Gene transcript levels were normalized against the geometric mean of 3 reference genes (*pgk1*, *ppia*, and *hgprt*). Relative expression, *P*-values and 95% CIs were calculated using the REST2009 software (Qiagen), which incorporates Ct and efficiency values determined by qPCR analysis. *Arc*, activity-regulated cytoskeleton-associated protein; Cb, cerebellum; Ctx, cortex; Hippo, hippocampus; *hprt*, hypoxanthine-guanine phosphoribosyl transferase; *mbp*, myelin basic protein; *nrgn*, RC3/neurogranin; *pgk1*, phosphoglycerate kinase 1; *ppia*, peptidylprolyl isomerase A; *ppp1r9b*, spinophilin.

racemic PCB 95 and PCB 136 are potent sensitizers of RyRs *in vitro*, with comparable potencies and efficacies towards activation of RyR1 (Pessah *et al.*, 2006). Moreover, chiral PCBs enantioselectively affect cellular targets involved in intracellular Ca^{2+} signaling (Lehmler *et al.*, 2005; Pessah *et al.*, 2009) and, as we have shown for PCB 136 atropisomers, enantioselectively alter neuronal connectivity in primary neurons *via* RyR-dependent mechanisms (Yang *et al.*, 2014). The toxicological relevance of the enantiomeric enrichment of RyR-active PCBs is further underscored by reports of variable enantiomeric enrichment of PCBs in human samples, including brain tissue (reviewed in: Kania-Korwel and Lehmler, 2016b).

Like the parent PCBs, OH-PCBs affect a range of cellular targets and are developmental neurotoxicants (Grimm *et al.*, 2015; Pessah *et al.*, 2010). For example, OH-PCBs of PCB 95 and PCB 136 are potent sensitizers and/or uncouplers of RyRs (Niknam *et al.*, 2013; Pessah *et al.*, 2006). Moreover, OH-PCBs with *ortho* chlorine substituents affect developmental neurotoxicity endpoints, such as microsomal Ca^{2+} sequestration and protein kinase C (PKC) translocation *in vitro* (Kodavanti *et al.*, 2003). OH-PCBs also cause endocrine and thyroid disruption (reviewed in: Grimm *et al.*, 2015) as well as oxidative stress (Dreiem *et al.*, 2009). To advance our understanding of the role of OH-PCBs in the developmental neurotoxicity of PCBs, we assessed the enantioselective disposition of potentially neurotoxic OH-PCBs in developmentally exposed pups. We observed complex OH-PCB mixtures that varied according to the congener, tissue and time point investigated, and between pups and dams. Changes in the expression of drug metabolizing enzymes, such as P450 enzymes, during early development and following PCB exposure are a likely explanation for the differences in OH-PCB profiles. The later hypothesis is supported by moderate, but statistically significant differences in the expression of relevant P450 enzymes between experimental groups in this study. Particularly intriguing is the presence of multiple OH-PCBs in the brains of pups in this study. For both PCB 95 and PCB 136-exposed pups, the profiles of the respective RyR-active OH-PCB metabolites in the brain differed between P7 and P21 pups and their dams. This observation is important because, in contrast to the respective parent PCBs, certain OH-PCBs can uncouple RyR channel activity from binding partners and produce unregulated Ca^{2+} leak (Niknam *et al.*, 2013), which may differentially affect neuronal connectivity. We also noted a relative enrichment of ΣOH-PCB metabolites compared with the parent PCB in the brain of P7 pups following exposure to PCB 136, but not PCB 95, and atropisomeric enrichment of OH-PCB metabolites of PCB 95 in lactating mice and their offspring. The latter finding is in agreement with reports that OH-PCBs display considerable atropisomeric enrichment in rodent models (Kania-Korwel *et al.*, 2008b, 2012, 2015).

Preliminary screening of the expression of neural plasticity and thyroid hormone-responsive genes, including *arc*, *ppp1r9b*, *mbp*, and *nrgn*, in specific brain regions revealed different, sex-specific gene expression profiles for PCB 95- versus PCB 136-exposed pups compared with control animals. For example, PCB 95 exposure decreased expression of thyroid hormone-responsive genes in the hippocampus of female and male pups and in the cerebellum of female pups but had no effect on neural plasticity genes. In contrast, PCB 136 exposure resulted in more complex effects on the expression of both neural plasticity and thyroid hormone-responsive genes with both categories of genes being up- or down-regulated depending on sex and brain region. The effects of developmental PCB exposure on levels of *mbp*, *nrgn*, and *ppp1r9b* transcripts have been documented in postnatal rats, but the changes in expression of these genes observed in this study were not consistent with the earlier studies (Lein *et al.*, 2007; Zoeller *et al.*, 2000), possibly due to differences in exposure paradigm (individual congeners vs PCB mixtures) and species (mouse vs rat). As has been demonstrated for PCB-exposed rats (Lein *et al.*, 2007), gene expression data do not necessarily predict morphological or behavioral changes associated with PCB exposure and represent only a preliminary assessment of the effects on PCB 95 versus PCB 136 on the developing brain. Together with the differences in PCB and PCB

metabolite profiles and chiral signatures in target tissues, our study raises 2 fundamental questions that warrant further studies: Do differences in the (enantioselective) metabolism of PCBs affect their developmental neurotoxicity? Are such differences in neurotoxic outcomes due to additive or more complex interactions produced by individual components of the complex PCB and OH-PCB mixtures present in the developing brain? The answers to these questions will have a significant impact on assessing the risk PCBs pose to the developing human brain, particularly in humans with genetic polymorphisms in cytochrome P450 metabolism and other drug metabolizing enzymes.

SUPPLEMENTARY DATA

Supplementary data are available at *Toxicological Sciences* online.

FUNDING

This work was supported by the National Institute of Environmental Health Science at the National Institute of Health (ES005605 and ES013661 to H-J.L., ES014901, ES023513 and ES011269 to P.J.L., ES017425 to H-J.L. and P.J.L., ES007059 to C.B.); U.S. Environmental Protection Agency (RD83543201 to P.J.L.); Natural Sciences and Engineering Research Council of Canada (14 April 2017 to S.M.B.); and Advancing Science in America (ARCS) Fellowship (to C.B.). The synthesis of metabolites of PCB 136 was supported by the National Institutes of Health (ES06694 to EA Mash and SC Waller of the Synthetic Chemistry Facility Core of the Southwest Environmental Health Sciences Center). The content is solely the responsibility of the authors and does not necessarily represent the official views of the funding agencies.

ACKNOWLEDGMENTS

We would like to thank Dr Sudhir N. Joshi, Dr Sandhya M. Vyas, Dr Yang Song, and Dr Huimin Wu for the synthesis of the PCB 95 metabolite standards. The PCB 136 metabolite standards were a generous gift from E.A. Mash and S.C. Waller of the Synthetic Chemistry Facility Core of the Southwest Environmental Health Sciences Center.

REFERENCES

Bal-Price, A., Lein, P. J., Keil, K. P., Sethi, S., Shafer, T., Barenys, M., Fritsche, E., Sachana, M., and Meek, M. E. (2017). Developing and applying the adverse outcome pathway concept for understanding and predicting neurotoxicity. *Neurotoxicology* **59**, 240–255.

Boix, J., Cauli, O., Leslie, H., and Felipo, V. (2011). Differential long-term effects of developmental exposure to polychlorinated biphenyls 52, 138 or 180 on motor activity and neurotransmission. Gender dependence and mechanisms involved. *Neurochem. Int.* **58**, 69–77.

Cauli, O., Piedrafita, B., Llansola, M., and Felipo, V. (2013). Gender differential effects of developmental exposure to methylmercury, polychlorinated biphenyls 126 or 153, or its combinations on motor activity and coordination. *Toxicology* **311**, 61–68.

Dreiem, A., Rykken, S., Lehmler, H. J., Robertson, L. W., and Fonnum, F. (2009). Hydroxylated polychlorinated biphenyls increase reactive oxygen species formation and induce cell death in cultured cerebellar granule cells. *Toxicol. Appl. Pharmacol.* **240**, 306–313.

Dziennis, S., Yang, D., Cheng, J., Anderson, K. A., Alkayed, N. J., Hurn, P. D., and Lein, P. J. (2008). Developmental exposure to polychlorinated biphenyls influences stroke outcome in adult rats. *Environ. Health Perspect.* **116**, 474–480.

Grimm, F. A., Hu, D., Kania-Korwel, I., Lehmler, H. J., Ludewig, G., Hornbuckle, K. C., Duffel, M. W., Bergman, A., and Robertson, L. W. (2015). Metabolism and metabolites of polychlorinated biphenyls. *Crit. Rev. Toxicol.* 245–272.

Guvenius, D. M., Aronsson, A., Ekman-Ordeberg, G., Bergman, Å., and Norén, K. (2003). Human prenatal and postnatal exposure to polybrominated diphenyl ethers, polychlorinated biphenyls, polychlorobiphenylols, and pentachlorophenol. *Environ. Health Perspect.* **111**, 1235–1241.

Hrycay, E., Forrest, D., Liu, L., Wang, R., Tai, J., Deo, A., Ling, V., and Bandiera, S. (2014). Hepatic bile acid metabolism and expression of cytochrome P450 and related enzymes are altered in Bsep$^{-/-}$ mice. *Mol. Cell. Biochem* **389**, 119–132.

Jacobson, J. L., and Jacobson, S. W. (1996). Intellectual impairment in children exposed to polychlorinated biphenyls in utero. *N. Engl. J. Med.* **335**, 783–789.

Jamshidi, A., Hunter, S., Hazrati, S., and Harrad, S. (2007). Concentrations and chiral signatures of polychlorinated biphenyls in outdoor and indoor air and soil in a major U.K. conurbation. *Environ. Sci. Technol.* **41**, 2153–2158.

Joshi, S. N., Vyas, S. M., Duffel, M. W., Parkin, S., and Lehmler, H. J. (2011). Synthesis of sterically hindered polychlorinated biphenyl derivatives. *Synthesis* **7**, 1045–1054.

Kania-Korwel, I., Barnhart, C. D., Lein, P. J., and Lehmler, H.-J. (2015). Effect of pregnancy on the disposition of 2,2′,3,5′,6-pentachlorobiphenyl (PCB 95) atropisomers and their hydroxylated metabolites in female mice. *Chem. Res. Toxicol.* **28**, 1774–1783.

Kania-Korwel, I., Barnhart, C. D., Stamou, M., Truong, K. M., El-Komy, M. H., Lein, P. J., Veng-Pedersen, P., and Lehmler, H.-J. (2012). 2,2′,3,5′,6-Pentachlorobiphenyl (PCB 95) and its hydroxylated metabolites are enantiomerically enriched in female mice. *Environ. Sci. Technol.* **46**, 11393–11401.

Kania-Korwel, I., Duffel, M. W., and Lehmler, H. J. (2011). Gas chromatographic analysis with chiral cyclodextrin phases reveals the enantioselective formation of hydroxylated polychlorinated biphenyls by rat liver microsomes. *Environ. Sci. Technol.* **45**, 9590–9596.

Kania-Korwel, I., Hrycay, E. G., Bandiera, S., and Lehmler, H.-J. (2008a). 2,2′,3,3′,6,6′-Hexachlorobiphenyl (PCB 136) atropisomers interact enantioselectively with hepatic microsomal cytochrome P450 enzymes. *Chem. Res. Toxicol.* **21**, 1295–1303.

Kania-Korwel, I., and Lehmler, H. J. (2016a). Chiral polychlorinated biphenyls: Absorption, metabolism and excretion-a review. *Environ. Sci. Pollut. Res. Int.* **23**, 2042–2057.

Kania-Korwel, I., and Lehmler, H. J. (2016b). Toxicokinetics of chiral polychlorinated biphenyls across different species-a review. *Environ. Sci. Pollut. Res. Int.* **23**, 2058–2080.

Kania-Korwel, I., Shaikh, N. S., Hornbuckle, K. C., Robertson, L. W., and Lehmler, H.-J. (2007). Enantioselective disposition of PCB 136 (2,2′,3,3′,6,6′-hexachlorobiphenyl) in C57BL/6 mice after oral and intraperitoneal administration. *Chirality* **19**, 56–66.

Kania-Korwel, I., Vyas, S. M., Song, Y., and Lehmler, H. J. (2008b). Gas chromatographic separation of methoxylated polychlorinated biphenyl atropisomers. *J. Chromatogr. A* **1207**, 146–154.

Kim, J. H., and Huganir, R. L. (1999). Organization and regulation of proteins at synapses. *Curr. Opin. Cell Biol.* **11**, 248–254.

Kodavanti, P. R. S., and Curras-Collazo, M. C. (2010). Neuroendocrine actions of organohalogens: Thyroid hormones, arginine vasopressin, and neuroplasticity. *Front. Neuroendocrinol.* **31**, 479–496.

Kodavanti, P. R. S., Ward, T. R., Derr-Yellin, E. C., McKinney, J. D., and Tilson, H. A. (2003). Increased [^{3}H]phorbol ester binding in rat cerebellar granule cells and inhibition of $^{45}Ca^{2+}$ buffering in rat cerebellum by hydroxylated polychlorinated biphenyls. *Neurotoxicology* **24**, 187–198.

Korrick, S. A., and Sagiv, S. K. (2008). Polychlorinated biphenyls, organochlorine pesticides and neurodevelopment. *Curr. Opin. Pediatr.* **20**, 198–204.

Krucker, T., Siggins, G. R., McNamara, R. K., Lindsley, K. A., Dao, A., Allison, D. W., De Lecea, L., Lovenberg, T. W., Sutcliffe, J. G., and Gerendasy, D. D. (2002). Targeted disruption of RC3 reveals a calmodulin-based mechanism for regulating metaplasticity in the hippocampus. *J. Neurosci.* **22**, 5525–5535.

Laemmli, U. K. (1970). Cleavage of structural proteins during the assembly of the head of bacteriophage T4. *Nature* **227**, 680–685.

Lehmler, H.-J., Harrad, S. J., Huhnerfuss, H., Kania-Korwel, I., Lee, C. M., Lu, Z., and Wong, C. S. (2010). Chiral polychlorinated biphenyl transport, metabolism, and distribution: A review. *Environ. Sci. Technol.* **44**, 2757–2766.

Lehmler, H.-J., Robertson, L. W., Garrison, A. W., and Kodavanti, P. R. S. (2005). Effects of PCB 84 enantiomers on [^{3}H] phorbol ester binding in rat cerebellar granule cells and $^{45}Ca^{2+}$-uptake in rat cerebellum. *Toxicol. Lett.* **156**, 391–400.

Lein, P. J., Yang, D., Bachstetter, A. D., Tilson, H. A., Harry, G. J., Mervis, R. F., and Kodavanti, P. R. S. (2007). Ontogenetic alterations in molecular and structural correlates of dendritic growth after developmental exposure to polychlorinated biphenyls. *Environ. Health Perspect.* 556–563.

Lesiak, A., Zhu, M., Chen, H., Appleyard, S. M., Impey, S., Lein, P. J., and Wayman, G. A. (2014). The environmental neurotoxicant PCB 95 promotes synaptogenesis via ryanodine receptor-dependent miR132 upregulation. *J. Neurosci.* **34**, 717–725.

Lu, Z., Kania-Korwel, I., Lehmler, H. J., and Wong, C. S. (2013). Stereoselective formation of mono- and dihydroxylated polychlorinated biphenyls by rat cytochrome P450 2B1. *Environ. Sci. Technol.* **47**, 12184–12192.

Lucier, G. W., McDaniel, O. S., Schiller, C. M., and Matthews, H. B. (1978). Structural requirements for the accumulation of chlorinated biphenyl metabolites in the fetal rat intestine. *Drug Metab. Dispos.* **6**, 584–590.

Meerts, I. A., Assink, Y., Cenijn, P. H., Van Den Berg, J. H., Weijers, B. M., Bergman, A., Koeman, J. H., and Brouwer, A. (2002). Placental transfer of a hydroxylated polychlorinated biphenyl and effects on fetal and maternal thyroid hormone homeostasis in the rat. *Toxicol. Sci.* **68**, 361–371.

Meerts, I. A. T. M., Hoving, S., van den Berg, J. H. J., Weijers, B. M., Swarts, H. J., van der Beek, E. M., Bergman, A., Koeman, J. H., and Brouwer, A. (2004a). Effects of in utero exposure to 4-hydroxy-2,3,3′,4′,5-pentachlorobiphenyl (4-OH-CB107) on developmental landmarks, steroid hormone levels, and female estrous cyclicity in rats. *Toxicol. Sci.* **82**, 259–267.

Meerts, I. A. T. M., Lilienthal, H., Hoving, S., van den Berg, J. H. J., Weijers, B. M., Bergman, A., Koeman, J. H., and Brouwer, A. (2004b). Developmental exposure to 4-hydroxy-2,3,3′,4′,5-pentachlorobiphenyl (4-OH-CB107): Long-term effects on brain development, behavior, and brain stem auditory evoked potentials in rats. *Toxicol. Sci.* **82**, 207–218.

Megson, D., O'Sullivan, G., Comber, S., Worsfold, P. J., Lohan, M. C., Edwards, M. R., Shields, W. J., Sandau, C. D., and Patterson, D. G. Jr. (2013). Elucidating the structural properties that influence the persistence of PCBs in humans using the National Health and Nutrition Examination Survey (NHANES) dataset. *Sci. Total Environ.* **461-462C**, 99–107.

Mitchell, M. M., Woods, R., Chi, L. H., Schmidt, R. J., Pessah, I. N., Kostyniak, P. J., and LaSalle, J. M. (2012). Levels of select PCB and PBDE congeners in human postmortem brain reveal possible environmental involvement in 15q11-q13 duplication autism spectrum disorder. *Environ. Mol. Mutagen.* **53**, 589–598.

Morse, D. C., Wehler, E. K., van de Pas, M., de Bie, A. T., van Bladeren, P. J., and Brouwer, A. (1995). Metabolism and biochemical effects of 3,3′,4,4′-tetrachlorobiphenyl in pregnant and fetal rats. *Chem. Biol. Interact.* **95**, 41–56.

Ngui, J. S., and Bandiera, S. M. (1999). Induction of hepatic CYP2B is a more sensitive indicatior of exposure to Aroclor 1260 than CYP1A in male rats. *Toxicol. Appl. Pharmacol.* **161**, 160–170.

Niknam, Y., Feng, W., Cherednichenko, G., Dong, Y., Joshi, S. N., Vyas, S. M., Lehmler, H.-J., and Pessah, I. N. (2013). Structure-activity relationship of select *meta*- and *para*-hydroxylated non-dioxin-like polychlorinated biphenyls: From single RyR1 channels to muscle dysfunction. *Toxicol. Sci.* **136**, 500–513.

Nowack, N., Wittsiepe, J., Kasper-Sonnenberg, M., Wilhelm, M., and Scholmerich, A. (2015). Influence of low-level prenatal exposure to PCDD/Fs and PCBs on empathizing, systemizing and autistic traits: Results from the Duisburg Birth Cohort Study. *PLoS One* **10**, e0129906.

Park, J.-S., Linderholm, L., Charles, M. J., Athanasiadou, M., Petrik, J., Kocan, A., Drobna, B., Trnovec, T., Bergman, A., and Hertz-Picciotto, I. (2007). Polychlorinated biphenyls and their hydroxylated metabolites (OH-PCBs) in pregnant women from Eastern Slovakia. *Environ. Health Perspect.* **115**, 20–27.

Pessah, I. N., Cherednichenko, G., and Lein, P. J. (2010). Minding the calcium store: Ryanodine receptor activation as a convergent mechanism of PCB toxicity. *Pharmacol. Ther.* **125**, 260–285.

Pessah, I. N., Hansen, L. G., Albertson, T. E., Garner, C. E., Ta, T. A., Do, Z., Kim, K. H., and Wong, P. W. (2006). Structure-activity relationship for noncoplanar polychlorinated biphenyl congeners toward the ryanodine receptor-Ca^{2+} channel complex type 1 (RyR1). *Chem. Res. Toxicol.* **19**, 92–101.

Pessah, I. N., Lehmler, H.-J., Robertson, L. W., Perez, C. F., Cabrales, E., Bose, D. D., and Feng, W. (2009). Enantiomeric specificity of (-)-2,2′,3,3′,6,6′-hexachlorobiphenyl toward ryanodine receptor types 1 and 2. *Chem. Res. Toxicol.* **22**, 201–207.

Santos, A. R., and Duarte, C. B. (2008). Validation of internal control genes for expression studies: Effects of the neurotrophin BDNF on hippocampal neurons. *J. Neurosci. Res.* **86**, 3684–3692.

SAS Institute (2013). *Base SAS® 9.4 Procedures Guide: Statistical Procedures*, 2nd edn. SAS Institute Inc., Cary, NC.

Schantz, S. L., Moshtaghian, J., and Ness, D. K. (1995). Spatial learning deficits in adult rats exposed to ortho-substituted PCB congeners during gestation and lactation. *Fundam. Appl. Toxicol.* **26**, 117–126.

Schantz, S. L., Seo, B.-W., Wong, P. W., and Pessah, I. N. (1997). Long-term effects of developmental exposure to 2,2′,3,5′,6-pentachlorobiphenyl (PCB 95) on locomotor activity, spatial learning and memory and brain ryanodine binding. *Neurotoxicology* **18**, 457–467.

Schecter, A., Colacino, J., Haffner, D., Patel, K., Opel, M., Papke, O., and Birnbaum, L. (2010). Perfluorinated compounds,

polychlorinated biphenyls, and organochlorine pesticide contamination in composite food samples from Dallas, Texas, USA. *Environ. Health Perspect.* **118**, 796–802.

Segal, M. (2001). New building blocks for the dendritic spine. *Neuron* **31**, 169–171.

Shin, E. S., Nguyen, K. H., Kim, J., Kim, C. I., and Chang, Y. S. (2015). Progressive risk assessment of polychlorinated biphenyls through a Total Diet Study in the Korean population. *Environ. Pollut.* **207**, 403–412.

Soechitram, S. D., Athanasiadou, M., Hovander, L., Bergman, A., and Sauer, P. J. J. (2004). Fetal exposure to PCBs and their hydroxylated metabolites in a Dutch cohort. *Environ. Health Perspect* **112**, 1208–1212.

Stamou, M., Uwimana, E., Flannery, B. M., Kania-Korwel, I., Lehmler, H. J., and Lein, P. J. (2015). Subacute nicotine coexposure has no effect on 2,2′,3,5′,6-pentachlorobiphenyl disposition but alters hepatic cytochrome P450 expression in the male rat. *Toxicology* **338**, 59–68.

Stamou, M., Wu, X., Kania-Korwel, I., Lehmler, H. J., and Lein, P. J. (2014). Cytochrome P450 mRNA expression in the rodent brain: Species-, sex-, and region-dependent differences. *Drug Metab. Dispos.* **42**, 239–244.

Thomas, K., Xue, J., Williams, R., Jones, P., and Whitaker, D. (2012). Polychlorinated biphenyls (PCBs) in school buildings: Sources, environmental levels, and exposures. United States Environmental Protection Agency, Office of Research and Development, National Exposure Research Laboratory. Available at: https://www.google.com/url?sa=t&rct=j&q=&esrc=s&source=web&cd=1&ved=0ahUKEwj6sYGRs6zTAhXI5iYKHVuaAVUQFggpMAA&url=https%3A%2F%2Fwww.epa.gov%2Fsites%2Fproduction%2Ffiles%2F2015-08%2Fdocuments%2Fpcb_epa600r12051_final.pdf&usg=AFQjCNEfy7NJXsc2snMM9-Ljmj66Nc9xlQ&cad=rja. Accessed April 17, 2017.

Towbin, H., Staehelin, T., and Gordon, J. (1979). Electrophoretic transfer of proteins from polyacrylamide gels to nitrocellulose sheets: Procedure and some applications. *Proc. Natl. Acad. Sci. U. S. A.* **76**, 4350–4354.

Uwimana, E., Li, X., and Lehmler, H.-J. (2016). 2,2′,3,5′,6-Pentachlorobiphenyl (PCB 95) is atropselectively metabolized to para-hydroxylated metabolites by human liver microsomes. *Chem. Res. Toxicol.* **29**, 2108–2110.

Waller, S. C., He, Y. A., Harlow, G. R., He, Y. Q., Mash, E. A., and Halpert, J. R. (1999). 2,2′,3,3′,6,6′-Hexachlorobiphenyl hydroxylation by active site mutants of cytochrome P450 2B1 and 2B11. *Chem. Res. Toxicol.* **12**, 690–699.

Wang, A., and Bandiera, S. (1996). Inductive effect of Telazol on hepatic expression of cytochrome P450 2B in rats. *Biochem. Pharmacol.* **52**, 735–742.

Warner, N. A., Martin, J. W., and Wong, C. S. (2009). Chiral polychlorinated biphenyls are biotransformed enantioselectively by mammalian cytochrome P-450 isozymes to form hydroxylated metabolites. *Environ. Sci. Technol.* **43**, 114–121.

Wayman, G. A., Bose, D. D., Yang, D., Lesiak, A., Bruun, D., Impey, S., Ledoux, V., Pessah, I. N., and Lein, P. J. (2012a). PCB-95 modulates the calcium-dependent signaling pathway responsible for activity-dependent dendritic growth. *Environ. Health Perspect.* **120**, 1003–1009.

Wayman, G. A., Yang, D., Bose, D. D., Lesiak, A., Ledoux, V., Bruun, D., Pessah, I. N., and Lein, P. J. (2012b). PCB-95 promotes dendritic growth via ryanodine receptor-dependent mechanisms. *Environ. Health Perspect.* **120**, 997–1002.

Whitcomb, B. W., Schisterman, E. F., Buck, G. M., Weiner, J. M., Greizerstein, H., and Kostyniak, P. J. (2005). Relative concentrations of organochlorines in adipose tissue and serum among reproductive age women. *Environ. Toxicol. Pharmacol.* **19**, 203–213.

Wingfors, H., Selden, A. I., Nilsson, C., and Haglund, P. (2006). Identification of markers for PCB exposure in plasma from Swedish construction workers removing old elastic sealants. *Ann. Occup. Hyg.* **50**, 65–73.

Wolff, M. S., Fischbein, A., and Selikoff, I. J. (1992). Changes in PCB serum concentrations among capacitor manufacturing workers. *Environ. Res.* **59**, 202–216.

Wu, X., Barnhart, C., Lein, P. J., and Lehmler, H. J. (2015). Hepatic metabolism affects the atropselective disposition of 2,2′,3,3′,6,6′-hexachlorobiphenyl (PCB 136) in mice. *Environ. Sci. Technol.* **49**, 616–625.

Wu, X., Duffel, M., and Lehmler, H.-J. (2013). Oxidation of polychlorinated biphenyls by liver tissue slices from phenobarbital-pretreated mice is congener-specific and atropselective. *Chem. Res. Toxicol.* **26**, 1642–1651.

Yang, D., Kania-Korwel, I., Ghogha, A., Chen, H., Stamou, M., Bose, D. D., Pessah, I. N., Lehmler, H. J., and Lein, P. J. (2014). PCB 136 atropselectively alters morphometric and functional parameters of neuronal connectivity in cultured rat hippocampal neurons via ryanodine receptor-dependent mechanisms. *Toxicol. Sci.* **138**, 379–392.

Yang, D., Kim, K. H., Phimister, A., Bachstetter, A. D., Ward, T. R., Stackman, R. W., Mervis, R. F., Wisniewski, A. B., Klein, S. L., Kodavanti, P. R., *et al.* (2009). Developmental exposure to polychlorinated biphenyls interferes with experience-dependent dendritic plasticity and ryanodine receptor expression in weanling rats. *Environ. Health Perspect.* **117**, 426–435.

Yang, H., and Wang, H. (2014). Signaling control of the constitutive androstane receptor (CAR). *Protein Cell* **5**, 113–123.

Zoeller, R. T., Dowling, A. L., and Vas, A. A. (2000). Developmental exposure to polychlorinated biphenyls exerts thyroid hormone-like effects on the expression of RC3/neurogranin and myelin basic protein messenger ribonucleic acids in the developing rat brain. *Endocrinology* **141**, 181–189.